NAVAL POSTGRADUATE SCHOOL
Monterey, California

THESIS

EVALUATION OF AND METHODS TO REDUCE CO-CHANNEL INTERFERENCE ON THE FORWARD CHANNEL OF A CDMA CELLULAR SYSTEM

by

Tanya G. Mayer

December 1998

Thesis Advisor: Tri T. Ha
Co-Advisor: R. Clark Robertson

REPORT DOCUMENTATION PAGE

Form Approved OMB No. 0704-0188

1. AGENCY USE ONLY *(Leave blank)*	2. REPORT DATE	3. REPORT TYPE AND DATES COVERED
	December 1998	Master's Thesis

4. TITLE AND SUBTITLE	5. FUNDING NUMBERS
Evaluation of and Methods to Reduce Co-Channel Interference on the Forward Channel of a CDMA Cellular System	
6. AUTHOR(S) Mayer, Tanya G.	
7. PERFORMING ORGANIZATION NAME(S) AND ADDRESS(ES) Naval Postgraduate School Monterey, CA 93943-5000	8. PERFORMING ORGANIZATION REPORT NUMBER
9. SPONSORING / MONITORING AGENCY NAME(S) AND ADDRESS(ES)	10. SPONSORING/MONITORING AGENCY REPORT NUMBER

11. SUPPLEMENTARY NOTES The views expressed in this thesis are those of the author and do not reflect the official policy or position of the Department of Defense or the U.S. Government.

12a. DISTRIBUTION / AVAILABILITY STATEMENT	12b. DISTRIBUTION CODE
Approved for public release; distribution is unlimited.	

13. ABSTRACT *(maximum 200 words)*

The large volumes of information necessary to support today's warfigher require the development of new technology to provide this type of secure, high data rate communication. The flexibility of cellular communications makes it an excellent choice for this purpose. Currently available cellular communications systems are narrowband; that is, they cannot support high data rate applications such as video, full Internet connection, and teleconferencing. Simply increasing the bandwidth of the existing systems will result in severe degradation due to frequency-selective fading, resulting in loss of quality and reliability. Instead, a new wideband cellular system can be used featuring a multicarrier, code division multiple access (CDMA) method. This type of system minimizes the effects of frequency-selective fading while reducing the probability of detection and interception. The limiting factor in this type of system is co-channel interference. This thesis focuses on analyzing the co-channel interference on the forward channel of the proposed CDMA cellular system and investigating methods such as sectoring and microzoning in an effort to reduce that interference.

14. SUBJECT TERMS	15. NUMBER OF PAGES
Cellular Communications, Co-Channel Interference, CDMA, Interference Reduction	98
	16. PRICE CODE

17. SECURITY CLASSIFICATION OF REPORT	18. SECURITY CLASSIFICATION OF THIS PAGE	19. SECURITY CLASSIFICATION OF ABSTRACT	20. LIMITATION OF ABSTRACT
Unclassified	Unclassified	Unclassified	UL

Approved for public release; distribution is unlimited

EVALUATION OF AND METHODS TO REDUCE CO-CHANNEL INTERFERENCE ON THE FORWARD CHANNEL OF A CDMA CELLULAR SYSTEM

Tanya G. Mayer
Lieutenant, United States Navy
B.S., United States Naval Academy, 1993

Submitted in partial fulfillment of the
requirements for the degree of

MASTER OF SCIENCE IN ELECTRICAL ENGINEERING

from the

NAVAL POSTGRADUATE SCHOOL
December 1998

ABSTRACT

The large volumes of information necessary to support today's warfigher require the development of new technology to provide this type of secure, high data rate communication. The flexibility of cellular communications makes it an excellent choice for this purpose. Currently available cellular communications systems are narrowband; that is, they cannot support high data rate applications such as video, full Internet connection, and teleconferencing. Simply increasing the bandwidth of the existing systems will result in severe degradation due to frequency-selective fading, resulting in loss of quality and reliability. Instead, a new wideband cellular system can be used featuring a multicarrier, code division multiple access (CDMA) method. This type of system minimizes the effects of frequency-selective fading while reducing the probability of detection and interception. The limiting factor in this type of system is co-channel interference. This thesis focuses on analyzing the co-channel interference on the forward channel of the proposed CDMA cellular system and investigating methods such as sectoring and microzoning in an effort to reduce that interference.

TABLE OF CONTENTS

LIST OF FIGURES

LIST OF TABLES

I. INTRODUCTION

A. HIGH DATA RATE CELLULAR SYSTEMS

There are two main developments creating the next major trend in the information age; they are the demand for greater mobility and more powerful data access. To support these demands toward the goal of true mobile multimedia, a third generation high data rate, wireless communication system is being developed. The requirements for this new system range from basic voice to high-speed data services. The data rates will range from 8 kbps to 384 kbps at the onset, with data rates eventually reaching 2 Mbps. Services will support applications such as full Internet access as well as mobile video teleconferencing.

B. CDMA IMPLEMENTATION FOR HIGH DATA RATE CELLULAR

Currently available cellular communications systems are narrowband; that is, they cannot support high data rate applications such as video, full Internet connection, and teleconferencing. Simply increasing the bandwidths of the existing systems will result in severe degradation due to frequency-selective fading, resulting in loss of quality and reduced reliability. Instead, a new wideband cellular system can be used featuring multicarrier, code division multiple access (CDMA). This type of system utilizes site diversity and exploits multipath fading through Rake combining, while reducing the probability of detection and interception. [1] Another benefit of CDMA is that there is no need to perform frequency/code planning in some cases. This will be explained in greater detail in Chapters II and IV.

When implementing a cellular architecture with CDMA, the signal-to-interference plus noise ratio (S/N) determines the quality of service experienced by the user. Co-channel interference is the limiting factor in a cellular mobile radio system [2]. This thesis will examine the S/N ratio due to additive white Gaussian noise (AWGN), intra-cell interference, and co-channel interference for several different types of cellular architectures using CDMA. Intra-cell interference is defined as the interference generated by other users within the reference cell operating on the same frequency band as the desired user. Co-channel interference will be explained in the next section.

During the course of studying different techniques for lowering co-channel interference, it became clear that a previously published method known as microzoning was incorrectly analyzed in several references. [3][4] The correct analysis of the microzoning technique for a narrowband FDMA (frequency-division multiple access) system is presented in this thesis, and the analysis is extended to the use of microzoning in a CDMA system.

C. FREQUENCY-REUSE AND CO-CHANNEL INTERFERENCE

One of the main design considerations of a cellular system is the frequency-reuse pattern. The ability of several cells to use the same set of frequencies is one of the primary factors in determining the system's capacity. In a traditional FDMA system, the total number of cells that collectively use the entire system's spectrum is called a cluster. Cells that share the same set of frequencies are known as co-channel cells. Because of their frequency sharing, co-channel cells create interference with each other. This interference is a function of distance as well as transmitted power levels. [3]

Frequency-reuse in the terms described above is most commonly associated with FDMA and TDMA systems where each cell is allocated a portion of the available bandwidth. A frequency in use in one cell may be reused in another cell sufficiently far away so that the interference is not significant. To extend this idea to CDMA systems, the available spectrum is divided into sub-bands with the number of sub-bands being equal to the number of cells per cluster. Each set of co-channel cells is then allocated a particular frequency band. In this way, CDMA systems employing higher reuse patterns can be considered hybrid CDMA-FDMA systems. The process of increasing the number of cells per cluster, and thereby decreasing the co-channel interference, does have associated disadvantages. These disadvantages can manifest themselves in one of two ways: reduced data rate or reduced processing gain. Since a reduction in processing gain results in severe degradation of the S/N in a system with all other parameters being equal, the most plausible implementation of a higher reuse pattern system would be one in which the processing gain is kept constant and the data rate is reduced.

D. INTERFERENCE REDUCTION METHODS

In addition to the analysis of the one-cell per cluster omnidirectional antenna typically associated with a CDMA system, several methods will be introduced and examined in an effort to reduce co-channel interference, thereby allowing for greater system capacity. These methods are higher frequency-reuse patterns, sectoring, and microzoning.

It is worth mentioning that during the course of work on this thesis, parallel work was being conducted in industry toward a Third Generation Standard. There have been hints that sectoring may be considered as a method for lowering co-channel interference

in that standard; however, microzoning has not yet drawn any attention. [5] This thesis will present many compelling reasons to indicate that microzoning may be an excellent candidate for that standard.

II. CO-CHANNEL INTERFERENCE AND CELL SECTORING

A. SIGNAL-TO-NOISE PLUS INTERFERENCE RATIO DERIVATION

To derive an expression for the signal-to-noise plus interference ratio due to co-channel interference (S/N) in a CDMA system, several factors need to be considered: the number of users in the reference cell, the number of users in each of the co-channel cells, the AWGN present, the path loss exponents for each of the cells, and the ratio of interfering base stations' powers to the desired base station's power as received by the mobile. Potentially, all co-channel cells interfere with each other. However, in practice, only the first and second-tiers are analyzed since the interference from subsequent tiers is negligible as compared to the first- or first- and second-tiers.

The generalized expression for the S/N of either the forward or reverse link of a CDMA system is

$$\frac{S}{N}=\left[\left(\frac{Eb}{N_0}\right)^{-1}+\left(\frac{S}{I}\right)_{in-cell}^{-1}+\left(\frac{S}{I}\right)_{CCI-1}^{-1}+\left(\frac{S}{I}\right)_{CCI-2}^{-1}\right]^{-1} \tag{2.1}$$

where the four terms on the right-hand side will be defined in the following paragraph. This equation is an extension of one given by Rappaport [3]. This thesis will examine only the forward channel of the cellular system.

In equation 2.1, E_b/ N_o is the signal energy per bit-to-noise ratio, with N_o being the one-sided noise power spectral density, $E_b = P_oT_b$ the average energy per bit, T_b the bit duration, and P_o the power of the intended, or reference, base station.

For a CDMA system utilizing asynchronous PN codes for each user, the multiuser interference term within the reference cell is represented in equation 2.1 as [6]

$$\left(\frac{S}{I}\right)^{-1}_{in-cell} = \frac{2}{3N}\sum_{k=1}^{K_0-1}\frac{P_k}{P_0} \tag{2.2}$$

Here, N is the overall system processing gain, K_0 is the number of users in the reference cell, P_k is the average transmitted power from the reference base station to the users in the reference cell as received by the reference user, and P_o is the average transmitted power from the reference base station to the desired user in the reference cell. Within the framework of our CDMA system, Walsh-Hadamard (W-H) orthogonal spreading codes are used on the forward channel, effectively reducing the multiuser interference within the reference cell to zero for synchronous transmissions. [1]

Each cell's base station is assumed to transmit a unique PN code in addition to the W-H code unique to each user. Hence, the multiuser interference due to co-channels in the first-tier around the desired cell is approximated by

$$\left(\frac{S}{I}\right)^{-1}_{CCI-1} = \sum_{i=1}^{i_0}\frac{2}{3N}\left(\sum_{k=1}^{K_i}\frac{P_{ik}}{P_0}\right) \tag{2.3}$$

In this case, i_0 represents the number of first-tier co-channel cells, K_i is the number of users within the i^{th} co-channel cell, and P_{ik} represents the average transmitted power from the i^{th} co-channel's base station to the k^{th} user in that co-channel cell as received by the reference user.

The final term in the overall S/N expression is the second-tier co-channel multiuser interference, given by

$$\left(\frac{S}{I}\right)^{-1}_{CCI-2} = \sum_{i=1}^{j_0}\frac{2}{3N}\left(\sum_{k=1}^{K_j}\frac{P_{jk}}{P_0}\right) \tag{2.4}$$

In this case, j_0 represents the number of second-tier co-channel cells, K_j is the number of users within the j^{th} co-channel cell, and P_{jk} represents the average transmitted power from the j^{th} co-channel's base station to the k^{th} user in that co-channel cell as received by the reference user.

Assuming perfect power control at the base stations, we can simplify the power ratios in the S/N expression into distance ratios. The power from each co-channel cell is inversely proportional to the distance from the center of the co-channel cell to the reference mobile's location raised to the appropriate path loss exponent for that cell. Likewise, the power from the reference cell to the desired mobile is inversely proportional to the distance from the center of the reference cell to the reference mobile's location, raised to the path loss exponent for the reference cell.

B. MOBILE USER LOCATION

For a worst case analysis, the mobile unit is located on its reference cell's boundary. Although the cell boundary is any point on the perimeter of the cell, for purposes of this thesis, the boundary is considered to be at the farthest location from the center of the cell to truly represent the worst case. As such, the cell radius R is the distance from the center of the cell to any of the six vertices of the cell, where each cell is assumed to be hexagonal.

C. OMNIDIRECTIONAL AND SECTORING ANTENNAS

There are several different cellular system configurations possible. The simplest method of evaluation is to consider that the base station's transmitter is using an omnidirectional antenna, whereby one antenna, located at or near the center of the cell,

radiates to all users in a particular cell. Another method employed by cellular systems that may decrease co-channel interference is sectoring. Sectoring is the replacement of the base station's single omnidirectional antenna with several antennas, each transmitting to a certain sector of the cell. Within the context of an FDMA sectoring system, a cell experiences interference from only a fraction of the total number of co-channel cells. [3] Within the context of a CDMA sectoring system, a cell experiences interference from each of the co-channel cells, however, that interference will only be from a fraction of the total number of users within each of those co-channel cells. Sectoring patterns are normally implemented with either three 120° antennas or six 60° antennas.

D. EFFECTS OF SECTORING

In a traditional FDMA system, one of the disadvantages of cell sectoring is that the process of assigning a set of frequencies to each sector decreases the system capacity by the same amount as if that set of frequencies had been designated for distinct cells. Another way to look at it is that the total number of accessible channels in each cell are divided and assigned to an individual antenna. This reduces the available channels per cell by a factor of three for a 120° sectoring layout and a factor of six for a 60° sectoring layout, decreasing system capacity [3][4].

However, within the context of a CDMA system, sectoring has a slightly different effect. Because CDMA systems are power limited and not bandwidth limited, there are more available channels, or codes, than can be utilized in an omnidirectional layout. In other words, due to interference, the omnidirectional system reaches the number of users it can effectively accommodate before the number of unique codes is exhausted. If we let N be the number of available orthogonal spreading codes on the forward link per cell, we

should be able to accommodate close to N different users per cell considering only the limitations imposed by bandwidth. (There are typically 128 total codes on the forward channel of the envisioned third generation wireless systems; however, since a few of the channels are utilized for overhead purposes such as pilot tone, paging, and synchronization, we will consider N to be the number of codes available for user assignment, which is generally 125.) [1]. Integrating the concept of sectoring with CDMA power limitations, we see that the decrease in trunking efficiency experienced in the FDMA type of sectoring will still be a factor in a CDMA system. In this fashion, the trunking efficiency of the CDMA system is reduced by a factor of three for a 120° sectoring architecture and a factor of six for a 60° sectoring architecture, just as in the FDMA case. This means that the 120° sectoring reaches its bandwidth-imposed maximum at N/3 users, while the 60° sectoring system reaches its maximum number of users at N/6.

In the FDMA sense of sectoring, the base station has to switch the antenna and the frequency when a mobile travels from one sector to another within a cell. Similarly in the CDMA case, the base station has to switch the antenna when the mobile moves from sector to sector. This type of switching is known as hard hand-off.

E. WORST CASE SIGNAL-TO-NOISE PLUS INTERFERENCE ANALYSIS

This chapter will present the analysis for the worst-case scenarios of one-cell per cluster, three-cell per cluster, and seven-cell per cluster CDMA layouts. Omnidirectional antenna use, 120° sectoring, and 60° sectoring will be compared for each frequency-reuse pattern. Both first-tier and first- and second-tier co-channel interference will be examined for each of the above cases. Distances for this analysis will be given in terms

of R, the cell radius. Universally adopted hexagonal cell shapes will be used for the analysis.

1. One-cell per Cluster with Omnidirectional Antenna

The first layout is a one-cell per cluster, omnidirectional antenna system as seen in Figure 2.1 below.

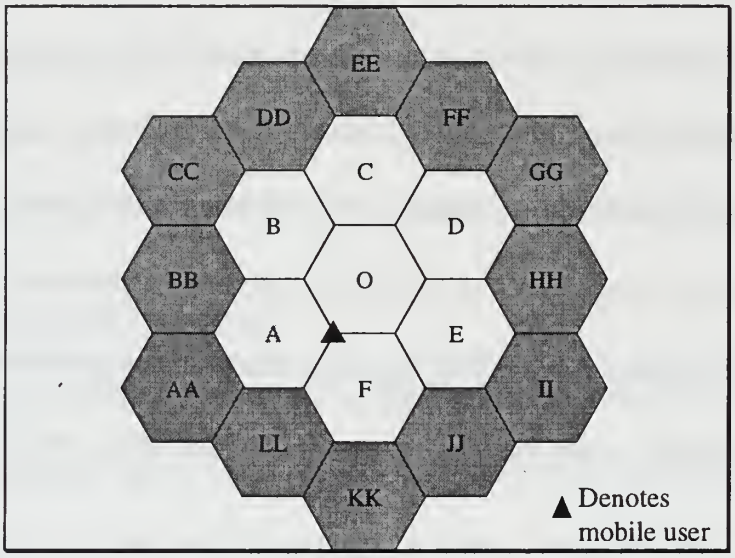

Figure 2.1: First- and Second-tier Co-channel Cells for a One-cell per Cluster, Omnidirectional Antenna System.

The reference cell, cell O, is the center cell. The immediately surrounding cells are the first-tier interfering cells, denoted by labels A through F. The second-tier co-channel cells, shaded in gray, are denoted by labels AA through LL. The first-tier multiuser co-channel interference term for a mobile on its cell boundary is given by

$$\left(\frac{S}{I}\right)^{-1}_{CCI-1} = \frac{2}{3N}\left[\frac{K_A(R)^{-n_A} + K_B(2R)^{-n_B} + K_C(\sqrt{7}R)^{-n_C}}{R^{-n_0}} + \frac{K_D(\sqrt{7}R)^{-n_D} + K_E(2R)^{-n_E} + K_F(R)^{-n_F}}{R^{-n_0}}\right] \tag{2.5}$$

where K_A through K_F are the number of users in each of the six first-tier co-channel cells. The distances from the center of the six first-tier co-channel cells to the reference mobile unit are raised to their respective path loss exponents, n_A through n_F. The path loss exponent for the reference cell is n_0.

The first- and second-tier co-channel interference for the one-cell per cluster, omnidirectional antenna system, includes the first-tier interference term listed above, in addition to the second-tier interference term, which for a mobile on its cell boundary is given by

$$\left(\frac{S}{I}\right)^{-1}_{CCI-2} = \frac{2}{3N}\left[\frac{K_{AA}\left(\sqrt{7}R\right)^{-n_{AA}} + K_{BB}\left(\sqrt{7}R\right)^{-n_{BB}} + K_{CC}\left(\sqrt{13}R\right)^{-n_{CC}} + K_{DD}\left(\sqrt{13}R\right)^{-n_{DD}} + K_{EE}\left(\sqrt{19}R\right)^{-n_{EE}}}{(R)^{-n_0}} + \right.$$

$$\frac{K_{FF}(4R)^{-n_{FF}} + K_{GG}\left(\sqrt{19}R\right)^{-n_{GG}} + K_{HH}\left(\sqrt{13}R\right)^{-n_{HH}} + K_{II}\left(\sqrt{13}R\right)^{-n_{II}}}{(R)^{-n_0}} +$$

$$\left.\frac{K_{JJ}\left(\sqrt{7}R\right)^{-n_{JJ}} + K_{KK}\left(\sqrt{7}R\right)^{-n_{KK}} + K_{LL}(2R)^{-n_{LL}}}{(R)^{-n_0}}\right] \qquad (2.6)$$

Here K_{AA} through K_{LL} represent the number of users in each of the respective second-tier co-channel cells. The distances from the center of the second-tier co-channel cells to the reference mobile unit are raised to the path loss exponents, n_{AA} through n_{LL}, associated with their particular cell.

2. One-cell per Cluster with 120° Sectoring Antenna

In the one-cell per cluster architecture with 120° sectoring pattern, shown in Figure 2.2, the mobile unit is arbitrarily chosen to be under the control of the right-most sector of the reference cell. In an FDMA sectoring system, only two cells in the first-tier,

cells A and B, would radiate into the reference cell, while only five second-tier cells, cells AA through EE, would generate interference into the reference cell. In a CDMA system, all sectors of the cell are operating on the same frequency band, and although orthogonal spreading codes are used within each cell, interference from the co-channel cells will be, in general, received asynchronously by the desired mobile. In addition, each cell's forward channel utilizes a PN code unique to that cell. As a result, additional sectors will generate multiuser interference in the reference sector. In the first-tier of the one-cell per cluster 120° sectoring architecture, the right-most sector of cells A and B will generate interference into the reference sector. However, the bottom sectors of cells C and D, as well as the top sectors of cells E and F must also be included in the analysis. Although one sector of each co-channel cell generates interference into the reference sector in a CDMA system, only the fraction of users located in that sector will interfere.

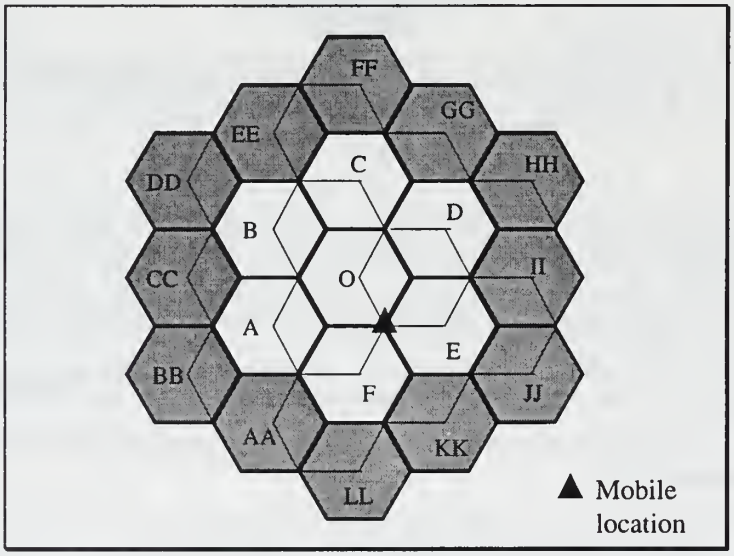

Figure 2.2: First- and Second-tier Co-channels for the One-cell per Cluster, 120° Sectoring Case.

The first-tier multiuser co-channel interference term at the worst case location is denoted by

$$\left(\frac{S}{I}\right)_{CCI-1}^{-1} = \frac{2}{3N}\left[\frac{\frac{K_A}{3}(2R)^{-n_A} + \frac{K_B}{3}\left(\sqrt{7}R\right)^{-n_B} + \frac{K_C}{3}\left(\sqrt{7}R\right)^{-n_C}}{R^{-n_0}} + \right.$$

$$\left. \frac{\frac{K_D}{3}(2R)^{-n_D} + \frac{K_E}{3}(R)^{-n_E} + \frac{K_F}{3}(R)^{-n_F}}{R^{-n_0}} \right] \tag{2.7}$$

Of note, in sectoring architectures, there will be co-channel interference due to only a fraction of the total number of users per cell. In the 120° sectoring scheme, there will only be, at most, one third of the total number of users per cell in each sector.

Continuing the analysis to include the co-channel interference due to the second-tier cells, we find that the signal-to-noise plus interference expression will include the previous first-tier interference term, the AWGN term, and the second-tier interference term given by

$$\left(\frac{S}{I}\right)_{CCI-2}^{-1} = \frac{2}{3N}\left[\frac{\frac{K_{AA}}{3}\left(\sqrt{7}R\right)^{-n_{AA}} + \frac{K_{BB}}{3}\left(\sqrt{13}R\right)^{-n_{BB}} + \frac{K_{CC}}{3}\left(\sqrt{13}R\right)^{-n_{CC}} + \frac{K_{DD}}{3}\left(\sqrt{19}R\right)^{-n_{DD}} + \frac{K_{EE}}{3}(4R)^{-n_{EE}}}{(R)^{-n_0}} + \right.$$

$$\frac{\frac{K_{FF}}{3}\left(\sqrt{19}R\right)^{-n_{FF}} + \frac{K_{GG}}{3}\left(\sqrt{13}R\right)^{-n_{GG}} + \frac{K_{HH}}{3}\left(\sqrt{13}R\right)^{-n_{HH}} + \frac{K_{II}}{3}\left(\sqrt{7}R\right)^{-n_{II}}}{(R)^{-n_0}} +$$

$$\left. \frac{\frac{K_{JJ}}{3}\left(\sqrt{7}R\right)^{-n_{JJ}} + \frac{K_{KK}}{3}(2R)^{-n_{KK}} + \frac{K_{LL}}{3}\left(\sqrt{7}R\right)^{-n_{LL}}}{(R)^{-n_0}} \right] \tag{2.8}$$

3. One-cell per Cluster with 60° Sectoring Antenna

The next case under consideration for the one-cell per cluster architecture is the 60° sectoring method as shown in Figure 2.3 below. In this scheme, there will only be co-channel interference due to, at most, one-sixth of the total number of users per cell.

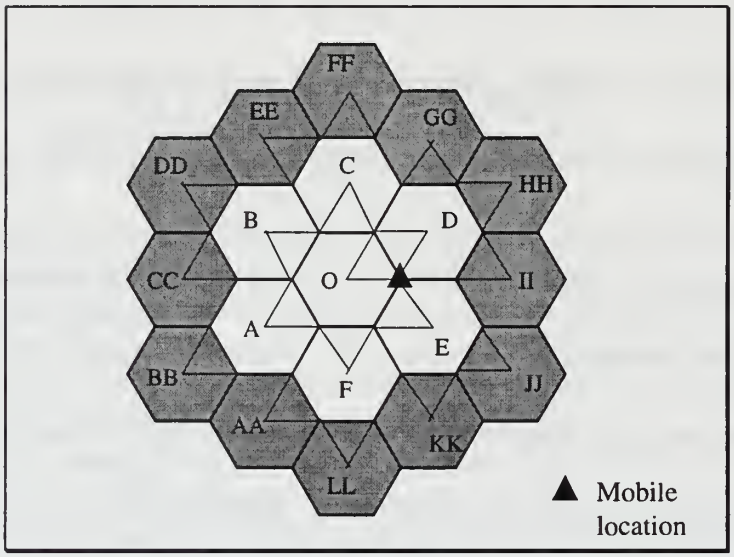

Figure 2.3: First- and Second-tier Co-channel Cells for a One-cell per Cluster, 60° Sectoring Case.

The first-tier interference ratio in the signal-to-noise plus interference expression is

$$\left(\frac{S}{I}\right)^{-1}_{CCI-1} = \frac{2}{3N}\left[\frac{\frac{K_A}{6}\left(\sqrt{7}R\right)^{-n_A} + \frac{K_B}{6}\left(\sqrt{7}R\right)^{-n_B} + \frac{K_C}{6}\left(2R\right)^{-n_C}}{R^{-n_0}} + \right.$$

$$\left. \frac{\frac{K_D}{6}\left(R\right)^{-n_D} + \frac{K_E}{6}\left(R\right)^{-n_E} + \frac{K_F}{6}\left(2R\right)^{-n_F}}{R^{-n_0}} \right] \qquad (2.9)$$

Extending the analysis to include the co-channel interference due to the second-tier co-channel cells, we find the second-tier co-channel interference term

$$\left(\frac{S}{I}\right)^{-1}_{CCI-2} = \frac{2}{3N}\left[\frac{\frac{K_{AA}}{6}\left(\sqrt{13}R\right)^{-n_{AA}} + \frac{K_{BB}}{6}\left(\sqrt{19}R\right)^{-n_{BB}} + \frac{K_{CC}}{6}\left(4R\right)^{-n_{CC}} + \frac{K_{DD}}{6}\left(\sqrt{19}R\right)^{-n_{DD}} + \frac{K_{EE}}{6}\left(\sqrt{13}R\right)^{-n_{EE}}}{\left(R\right)^{-n_0}} + \right.$$

$$\frac{\frac{K_{FF}}{6}\left(\sqrt{13}R\right)^{-n_{FF}} + \frac{K_{GG}}{6}\left(\sqrt{7}R\right)^{-n_{GG}} + \frac{K_{HH}}{6}\left(\sqrt{7}R\right)^{-n_{HH}} + \frac{K_{II}}{6}\left(2R\right)^{-n_{II}}}{\left(R\right)^{-n_0}} +$$

$$\left.\frac{\frac{K_{JJ}}{6}\left(\sqrt{7}R\right)^{-n_{JJ}} + \frac{K_{KK}}{6}\left(\sqrt{7}R\right)^{-n_{KK}} + \frac{K_{LL}}{6}\left(\sqrt{13}R\right)^{-n_{LL}}}{\left(R\right)^{-n_0}}\right] \qquad (2.10)$$

4. Three-cell per Cluster with Omnidirectional Antenna

The next architecture under study is the three-cell per cluster layout. Omnidirectional, 120° sectoring, and 60° sectoring antenna patterns will be examined for this architecture. The first case is the omnidirectional system as seen in Figure 2.4 below.

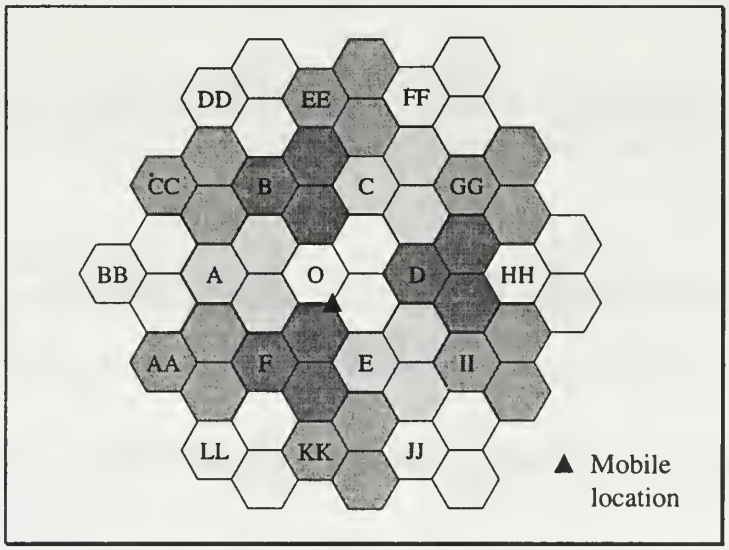

Figure 2.4: First- and Second-tier Co-channel Sells for a Three-cell per Cluster, Omnidirectional Antenna System.

In this figure, the first-tier interfering cells are labeled A through F and are shown as the leftmost cells within their parent clusters. The second-tier interfering cells are labeled AA

through LL and also appear as the leftmost cells within their clusters. The reference cell, labeled cell O, is colorless and is the leftmost cell in the center cluster. The mobile unit is shown in the worst-case location for interference purposes.

The first-tier co-channel interference term for the three-cell per cluster, omnidirectional system is given by

$$\left(\frac{S}{I}\right)_{CCI-1}^{-1} = \frac{2}{3N}\left[\frac{K_A\left(\sqrt{13}R\right)^{-n_A} + K_B(4R)^{-n_B} + K_C\left(\sqrt{13}R\right)^{-n_C}}{R^{-n_0}} + \right.$$

$$\left. \frac{K_D\left(\sqrt{7}R\right)^{-n_D} + K_E(2R)^{-n_E} + K_F\left(\sqrt{7}R\right)^{-n_F}}{R^{-n_0}}\right] \tag{2.11}$$

Extending the analysis to include the co-channel interference due to the second-tier interfering cells, we obtain the second-tier interference term

$$\left(\frac{S}{I}\right)_{CCI-2}^{-1} = \frac{2}{3N}\left[\frac{K_{AA}\left(\sqrt{28}R\right)^{-n_{AA}} + K_{BB}\left(\sqrt{43}R\right)^{-n_{BB}} + K_{CC}\left(\sqrt{37}R\right)^{-n_{CC}} + K_{DD}(7R)^{-n_{DD}} + K_{EE}\left(\sqrt{37}R\right)^{-n_{EE}}}{(R)^{-n_0}} + \right.$$

$$\frac{K_{FF}\left(\sqrt{43}R\right)^{-n_{FF}} + K_{GG}\left(\sqrt{28}R\right)^{-n_{GG}} + K_{HH}\left(\sqrt{81}R\right)^{-n_{HH}} + K_{II}\left(\sqrt{19}R\right)^{-n_{II}}}{(R)^{-n_0}} +$$

$$\left. \frac{K_{JJ}\left(\sqrt{7}R\right)^{-n_{JJ}} + K_{KK}\left(\sqrt{19}R\right)^{-n_{KK}} + K_{LL}\left(\sqrt{31}R\right)^{-n_{LL}}}{(R)^{-n_0}}\right] \tag{2.12}$$

5. Three-cell per Cluster with 120 ° Sectoring Antenna

A three-cell per cluster architecture with a 120 ° sectoring pattern is shown in Figure 2.5.

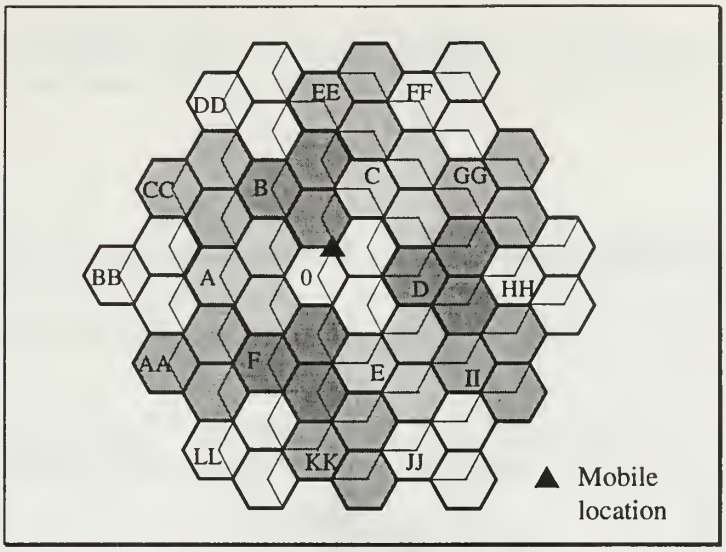

Figure 2.5: First- and Second-tier Co-channel Cells for a Three-cell per Cluster, 120 ° Sectoring System.

The first-tier co-channel interference term at the worst case location for the three-cell per cluster, 120° sectoring scheme is

$$\left(\frac{S}{I}\right)_{CCI-1}^{-1} = \frac{2}{3N}\left[\frac{\frac{K_A}{3}\left(\sqrt{13}R\right)^{-n_A} + \frac{K_B}{3}\left(\sqrt{7}R\right)^{-n_B} + \frac{K_C}{3}\left(2R\right)^{-n_C}}{R^{-n_0}} + \right.$$

$$\left. \frac{\frac{K_D}{3}\left(\sqrt{7}R\right)^{-n_D} + \frac{K_E}{3}\left(\sqrt{13}R\right)^{-n_E} + \frac{K_F}{3}\left(4R\right)^{-n_F}}{R^{-n_0}} \right] \tag{2.13}$$

To account for the second-tier interfering cells, the signal-to-noise plus interference ratio at the worst case location also includes the following second-tier term

$$\left(\frac{S}{I}\right)_{CCI-2}^{-1} = \frac{2}{3N}\left[\frac{\frac{K_{AA}}{3}\left(\sqrt{37}R\right)^{-n_{AA}} + \frac{K_{BB}}{3}\left(\sqrt{43}R\right)^{-n_{BB}} + \frac{K_{CC}}{3}\left(\sqrt{28}R\right)^{-n_{CC}} + \frac{K_{DD}}{3}\left(\sqrt{31}R\right)^{-n_{DD}} + \frac{K_{EE}}{3}\left(\sqrt{19}R\right)^{-n_{EE}}}{\left(R\right)^{-n_0}} + \right.$$

$$\left. \frac{\frac{K_{FF}}{3}\left(5R\right)^{-n_{FF}} + \frac{K_{GG}}{3}\left(\sqrt{19}R\right)^{-n_{GG}} + \frac{K_{HH}}{3}\left(\sqrt{31}R\right)^{-n_{HH}} + \frac{K_{II}}{3}\left(\sqrt{28}R\right)^{-n_{II}}}{\left(R\right)^{-n_0}} + \right.$$

$$\frac{\frac{K_{JJ}}{3}\left(\sqrt{43}R\right)^{-n_{JJ}}+\frac{K_{KK}}{3}\left(\sqrt{37}R\right)^{-n_{KK}}+\frac{K_{LL}}{3}(7R)^{-n_{LL}}}{(R)^{-n_0}}\Bigg] \tag{2.14}$$

6. Three-cell per Cluster with 60° Sectoring Antenna

A three-cell per cluster architecture with a 60° sectoring scheme is seen in Figure 2.6.

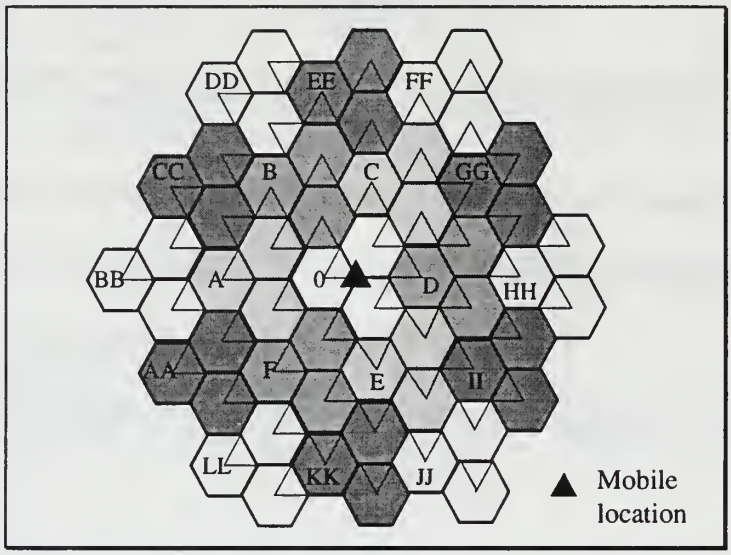

Figure 2.6: First- and Second-tier Co-channel Cells for a Three-cell per Cluster, 60° Sectoring Case.

The first-tier co-channel interference term is

$$\left(\frac{S}{I}\right)_{CCI-1}^{-1}=\frac{2}{3N}\Bigg[\frac{\frac{K_A}{6}\left(4R\right)^{-n_A}+\frac{K_B}{6}\left(\sqrt{13}R\right)^{-n_B}+\frac{K_C}{6}\left(\sqrt{7}R\right)^{-n_C}}{R^{-n_0}}+$$

$$\frac{\frac{K_D}{6}\left(2R\right)^{-n_D}+\frac{K_E}{6}\left(\sqrt{7}R\right)^{-n_E}+\frac{K_F}{6}\left(\sqrt{13}R\right)^{-n_F}}{R^{-n_0}}\Bigg] \tag{2.15}$$

The second-tier interference term is given by

$$\left(\frac{S}{I}\right)^{-1}_{CCI-2} = \frac{2}{3N}\left[\frac{\frac{K_{AA}}{6}\left(\sqrt{37}R\right)^{-n_{AA}} + \frac{K_{BB}}{6}\left(7R\right)^{-n_{BB}} + \frac{K_{CC}}{6}\left(\sqrt{37}R\right)^{-n_{CC}} + \frac{K_{DD}}{6}\left(\sqrt{43}R\right)^{-n_{DD}} + \frac{K_{EE}}{6}\left(\sqrt{28}R\right)^{-n_{EE}}}{\left(R\right)^{-n_0}} + \right.$$

$$\frac{\frac{K_{FF}}{6}\left(\sqrt{31}R\right)^{-n_{FF}} + \frac{K_{GG}}{6}\left(\sqrt{19}R\right)^{-n_{GG}} + \frac{K_{HH}}{6}\left(5R\right)^{-n_{HH}} + \frac{K_{II}}{6}\left(\sqrt{19}R\right)^{-n_{II}}}{\left(R\right)^{-n_0}} +$$

$$\left.\frac{\frac{K_{JJ}}{6}\left(\sqrt{31}R\right)^{-n_{JJ}} + \frac{K_{KK}}{6}\left(\sqrt{28}R\right)^{-n_{KK}} + \frac{K_{LL}}{6}\left(\sqrt{43}R\right)^{-n_{LL}}}{\left(R\right)^{-n_0}}\right] \qquad (2.16)$$

7. Seven-cell per Cluster with Omnidirectional Antenna

The next architecture for analysis is the seven-cell per cluster layout. Omnidirectional, 120° sectoring, and 60° sectoring antenna patterns will be examined for this architecture. The first case is the omnidirectional antenna as seen in Figure 2.7. The first-tier interfering cells are labeled A through F and are shown as the center cells of their parent clusters. The second-tier interfering cells are labeled AA through LL and are also the center cells in their respective clusters. The reference cell is labeled O and the mobile unit is shown in the worst case location.

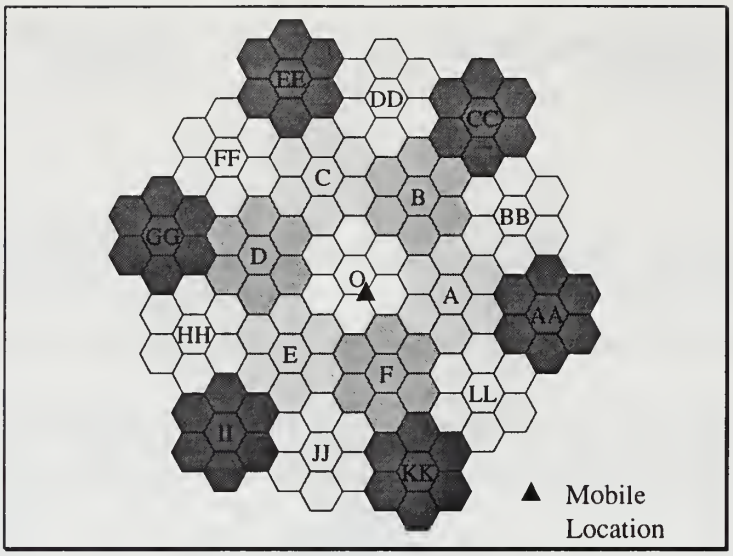

Figure 2.7: First- and Second-tier Co-channel Cells for a Seven-cell per Cluster, Omnidirectional Antenna System.

The first-tier interference term for the seven-cell per cluster, omnidirectional system is given by

$$\left(\frac{S}{I}\right)_{CCI-1}^{-1} = \frac{2}{3N}\left[\frac{K_A(4R)^{-n_A} + K_B(5R)^{-n_B} + K_C\left(\sqrt{31}R\right)^{-n_C}}{R^{-n_0}} + \right.$$

$$\left. \frac{K_D\left(\sqrt{28}R\right)^{-n_D} + K_E\left(\sqrt{19}R\right)^{-n_E} + K_F\left(\sqrt{13}R\right)^{-n_F}}{R^{-n_0}}\right] \qquad (2.17)$$

Extending the analysis to include the second-tier co-channel interference, we obtain the second-tier interference term

$$\left(\frac{S}{I}\right)_{CCI-2}^{-1} = \frac{2}{3N}\left[\frac{K_{AA}\left(\sqrt{73}R\right)^{-n_{AA}} + K_{BB}\left(\sqrt{61}R\right)^{-n_{BB}} + K_{CC}\left(\sqrt{91}R\right)^{-n_{CC}} + K_{DD}\left(\sqrt{76}R\right)^{-n_{DD}}}{(R)^{-n_0}} + \right.$$

$$\left. \frac{K_{EE}\left(\sqrt{103}R\right)^{-n_{EE}} + K_{FF}\left(\sqrt{79}R\right)^{-n_{FF}} + K_{GG}\left(\sqrt{97}R\right)^{-n_{GG}} + K_{HH}\left(\sqrt{67}R\right)^{-n_{HH}} + K_{II}\left(\sqrt{79}R\right)^{-n_{II}}}{(R)^{-n_0}} + \right.$$

$$\frac{K_{JJ}\left(\sqrt{52}R\right)^{-n_{JJ}} + K_{KK}\left(\sqrt{67}R\right)^{-n_{KK}} + K_{LL}\left(7R\right)^{-n_{LL}}}{\left(R\right)^{-n_0}}\Bigg] \tag{2.18}$$

8. Seven-cell per Cluster with 120° Sectoring Antenna

The next layout to be studied for the seven-cell per cluster architecture is the 120° sectoring scheme as seen in Figure 2.8.

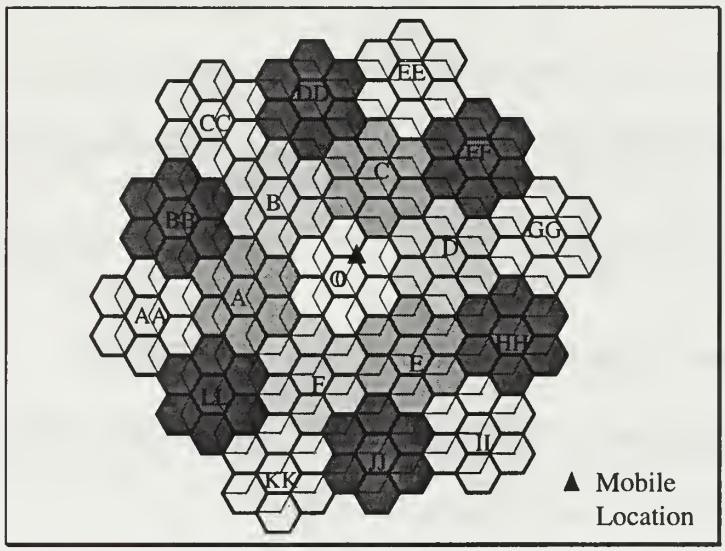

Figure 2.8: First- and Second-tier Co-channel Cells for a Seven-cell per Cluster, 120° Sectoring Case.

The first-tier co-channel interference term for the seven-cell per cluster, 120° sectoring scheme at the worst case location is

$$\left(\frac{S}{I}\right)^{-1}_{CCI-1} = \frac{2}{3N}\Bigg[\frac{\frac{K_A}{3}\left(\sqrt{28}R\right)^{-n_A} + \frac{K_B}{3}\left(\sqrt{19}R\right)^{-n_B} + \frac{K_C}{3}\left(\sqrt{13}R\right)^{-n_C}}{R^{-n_0}} + \frac{\frac{K_D}{3}\left(4R\right)^{-n_D} + \frac{K_E}{3}\left(5R\right)^{-n_E} + \frac{K_F}{3}\left(\sqrt{31}R\right)^{-n_F}}{R^{-n_0}}\Bigg] \tag{2.19}$$

To account for the second-tier interfering cells, the signal-to-noise plus interference ratio also includes the following second-tier interference term:

$$\left(\frac{S}{I}\right)^{-1}_{CCI-2} = \frac{2}{3N}\left[\frac{\frac{K_{AA}}{3}\left(\sqrt{97}R\right)^{-n_{AA}} + \frac{K_{BB}}{3}\left(\sqrt{67}R\right)^{-n_{BB}} + \frac{K_{CC}}{3}\left(\sqrt{79}R\right)^{-n_{CC}} + \frac{K_{DD}}{3}\left(\sqrt{52}R\right)^{-n_{DD}} + \frac{K_{EE}}{3}\left(\sqrt{67}R\right)^{-n_{EE}}}{(R)^{-n_0}} + \right.$$

$$\frac{\frac{K_{FF}}{3}\left(7R\right)^{-n_{FF}} + \frac{K_{GG}}{3}\left(\sqrt{73}R\right)^{-n_{GG}} + \frac{K_{HH}}{3}\left(\sqrt{61}R\right)^{-n_{HH}} + \frac{K_{II}}{3}\left(\sqrt{91}R\right)^{-n_{II}}}{(R)^{-n_0}} +$$

$$\left.\frac{\frac{K_{JJ}}{3}\left(\sqrt{76}R\right)^{-n_{JJ}} + \frac{K_{KK}}{3}\left(\sqrt{103}R\right)^{-n_{KK}} + \frac{K_{LL}}{3}\left(\sqrt{79}R\right)^{-n_{LL}}}{(R)^{-n_0}}\right] \qquad (2.20)$$

9. Seven-cell per Cluster with 60° Sectoring Antenna

The last case under consideration for the seven-cell per cluster architecture is the 60° sectoring method as seen in Figure 2.9 below.

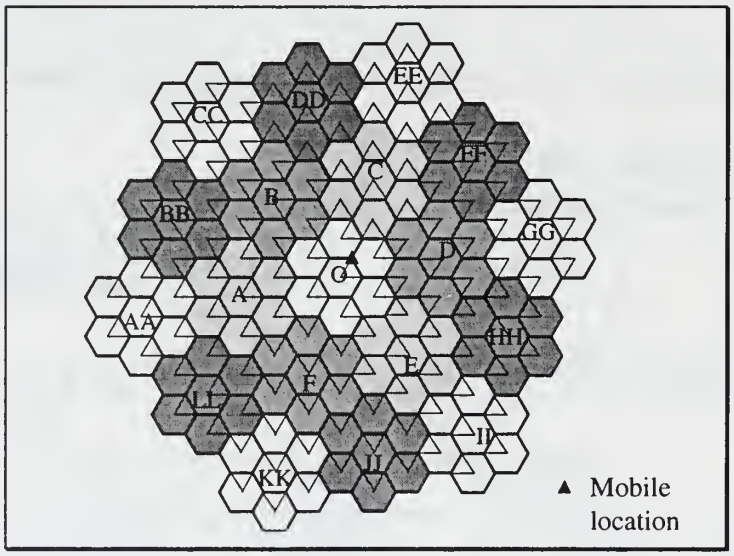

Figure 2.9: First- and Second-tier Co-channel Cells for a Seven-cell per Cluster, 60° Sectoring Case.

The first-tier co-channel interference term at the worst case location is

$$\left(\frac{S}{I}\right)_{CCI-1}^{-1} = \frac{2}{3N}\left[\frac{\frac{K_A}{6}\left(\sqrt{28}R\right)^{-n_A} + \frac{K_B}{6}\left(\sqrt{19}R\right)^{-n_B} + \frac{K_C}{6}\left(\sqrt{13}R\right)^{-n_C}}{R^{-n_0}} + \right.$$

$$\left.\frac{\frac{K_D}{6}\left(4R\right)^{-n_D} + \frac{K_E}{6}\left(5R\right)^{-n_E} + \frac{K_F}{6}\left(\sqrt{31}R\right)^{-n_F}}{R^{-n_0}}\right] \tag{2.21}$$

Extending the examination to include the co-channel interference due to the second-tier interferers as well, we get the following second-tier co-channel interference term

$$\left(\frac{S}{I}\right)_{CCI-2}^{-1} = \frac{2}{3N}\left[\frac{\frac{K_{AA}}{6}\left(\sqrt{97}R\right)^{-n_{AA}} + \frac{K_{BB}}{6}\left(\sqrt{67}R\right)^{-n_{BB}} + \frac{K_{CC}}{6}\left(\sqrt{79}R\right)^{-n_{CC}} + \frac{K_{DD}}{6}\left(\sqrt{52}R\right)^{-n_{DD}} + \frac{K_{EE}}{6}\left(\sqrt{67}R\right)^{-n_{EE}}}{\left(R\right)^{-n_0}} + \right.$$

$$\frac{\frac{K_{FF}}{6}\left(7R\right)^{-n_{FF}} + \frac{K_{GG}}{6}\left(\sqrt{73}R\right)^{-n_{GG}} + \frac{K_{HH}}{6}\left(\sqrt{61}R\right)^{-n_{HH}} + \frac{K_{II}}{6}\left(\sqrt{91}R\right)^{-n_{II}}}{\left(R\right)^{-n_0}} +$$

$$\left.\frac{\frac{K_{JJ}}{6}\left(\sqrt{76}R\right)^{-n_{JJ}} + \frac{K_{KK}}{6}\left(\sqrt{103}R\right)^{-n_{KK}} + \frac{K_{LL}}{6}\left(\sqrt{79}R\right)^{-n_{LL}}}{\left(R\right)^{-n_0}}\right] \tag{2.22}$$

F. SUMMARY

A quick reference for finding the first- and second-tier co-channel interference equations for each architecture is given in Table 2.1.

	One-cell per cluster	Three-cell per cluster	Seven-cell per cluster
First-tier Omnidirectional	Equation 2.5	Equation 2.11	Equation 2.17
Second-tier Omnidirectional	Equation 2.6	Equation 2.12	Equation 2.18
First-tier 120° sectoring	Equation 2.7	Equation 2.13	Equation 2.19
Second-tier 120° sectoring	Equation 2.8	Equation 2.14	Equation 2.20
First-tier 60° sectoring	Equation 2.9	Equation 2.15	Equation 2.21
Second-tier 60° sectoring	Equation 2.10	Equation 2.16	Equation 2.22

Table 2.1: Equation Reference for Chapter II Architectures

Now that the signal-to-noise plus interference ratios for all the combinations of one-cell, three-cell, and seven-cell per cluster architectures have been developed, a closer examination of performance can be accomplished. This comparison will be performed in the numerical analysis chapter by using specific values for path loss exponents, number of users per cell or sector, cell radius, signal bit energy-to-noise ratio (E_b / N_0), and overall system processing gain.

The next chapter will investigate the use of microzoning techniques for cellular systems and present derivations for the signal-to-noise plus interference ratios associated with those systems.

III. THE NARROWBAND MICROZONING CONCEPT

A. DEFINITION OF MICROZONING

Microzoning is a term used to describe a cellular system that has been divided into smaller zones, usually three. All the zones are fed by the equipment installed at the base station. Unlike the sectoring antennas analyzed in the previous chapter, the microzoning antennas are located at the edges of the each of the zones, and hence at the outer perimeter of the cell. Microzoning antennas also differ from sectoring antennas in that they radiate back toward the interior of their cells. Each zone has its own transmitter and receiver. The microzoning concept as presented by Rappaport and Lee is shown in Figure 3.1. The appropriate zone for each user is the zone that receives the mobile's signal the strongest. ' Only the appropriate zone transmits to a specific user at a time. [4]

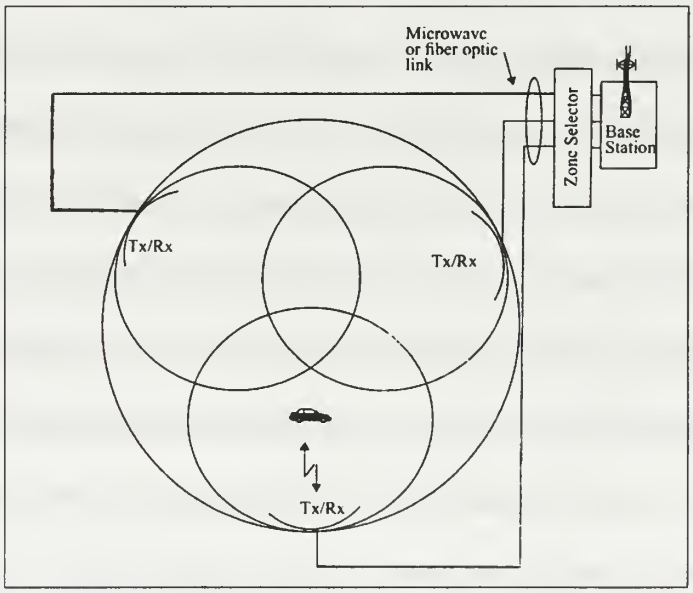

Figure 3.1: The Microzoning Concept [3].

As demonstrated in the last chapter, expressions for co-channel interference include the ratio of interfering base stations' powers to the desired base station's power as

received by the mobile. For the worst case analysis, we evaluate our mobile in a worst case location. Assuming perfect power control at the base stations, the power ratios can again be simplified into distance ratios. [3]

Lee's method for analyzing microzoning is presented in this chapter. His method attempts analysis of microzoning on a narrowband FDMA system, which will be shown to be inaccurate. Two methods, Mayer's method (version one) and Mayer's method (version two) are developed in this chapter to more accurately measure co-channel interference in a narrowband FDMA system. In addition, these two methods will be logically extended in Chapter IV to handle co-channel interference analysis using microzoning in CDMA systems.

As mentioned in Chapter II, the use of sectoring antennas effectively decreases the system capacity, or trunking efficiency, in an FDMA system. The advantage of microzoning is that when the mobile unit moves from zone to zone within a cell, it remains on the same assigned channel. Control of that channel is simply switched to the appropriate zone. There is no need for each zone to have its own separate set of channels from the other zones in the cell. As a result, capacity is dependent on the separation between the co-channel cells as in the omnidirectional case and hence, is not lowered as it is in the sectoring case. The soft hand-off from zone to zone experienced with the microzoning method is an advantage over the hard hand-off experienced with the sectoring method. The advantage stems from the reduction in system overhead associated with not having to re-acquire the signal with every zone change. [4]

B. LEE'S MICROZONING METHOD

The parameter used by Lee to gauge the microzone co-channel interference is the ratio of the distance between the two nearest zones of their parent co-channel cells to the radius of the zone. [4] That method of distance measurement is shown in Figure 3.2.

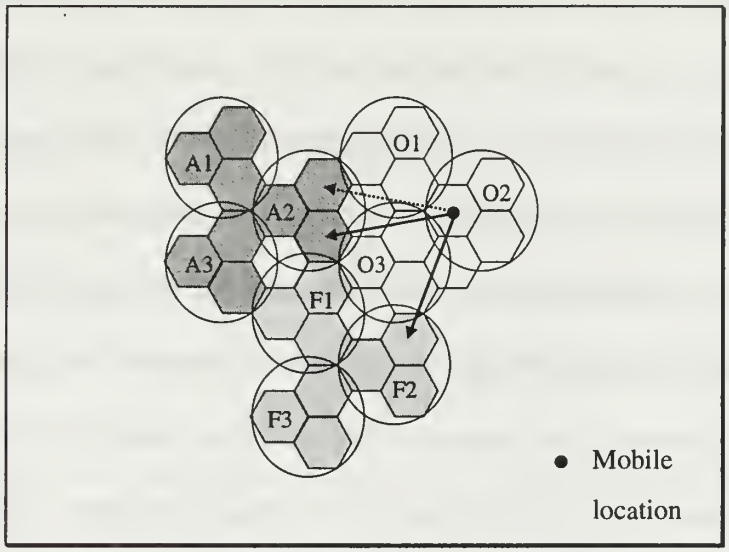

Figure 3.2: Lee's Method for Measuring Co-channel Distance.

In this illustration, a cutaway of a three-cell per cluster system is represented. The three clusters are designated as clusters O, A, and F which appear as the first letter of the cell labels. Each cluster is shown in a unique shade of gray. Every cluster has three cells, which are represented by circles and designated as cells 1, 2, and 3. They appear as the last number of the cell labels. As in the previous chapter, all cells designated with a one use the same set of frequencies, and hence, are co-channel interferers with each other. The same is true for cells designated as cell 2 of their cluster, as well as cells designated cell 3 of their cluster. Finally, each cell is divided into three zones, which are represented by the shaded hexagons circumscribed within each cell circle.

Lee's method of distance measurement for co-channel interference considers the mobile to be located at the center of the zone of interest, and hence uses the zone radius as the worst case location for the mobile to receive the desired zone's signal. In the figure, the mobile is located at the center of the leftmost zone in cell two of the original, reference cluster (cell O2). The co-channel distance to cluster A is measured from the mobile location to the center of the bottom zone of cell two in cluster A (cell A2). Of note, the distance to the bottom zone of cell A2 is the same as the distance to the top zone of cell A2, so either can be used with this method. The co-channel distance to cluster F is measured from the mobile location to the center of the top zone of cell F2. In this case, the topmost zone provides an outright closest distance and is the only zone considered in cell F2 with this method. Lee's method does not take into consideration the directivity of the microzone transmitters, which changes the co-channel distances. This issue will be addressed in sections 3.5 through 3.12 under Mayer's microzoning methods, versions one and two.

In the next three sections of this chapter, 3.2 through 3.4, will present the analysis using Lee's method for the one-cell per cluster, three-cell per cluster, and seven-cell per cluster microzoning layouts is presented. Equation 2.1 will be used for finding the signal-to-interference plus noise (S/N) ratio for all architectures presented in this chapter. The Gaussian noise term will remain the same as in the previous chapter. The multiuser interference term within the reference cell will also be equal to zero as in the previous chapter, but for a different reason. The orthogonal property of the Walsh-Hadamard spreading functions used on the forward channel in the CDMA system reduces the multiuser interference within the reference cell to zero. In an FDMA system, the

multiuser interference term within the reference cell is zero because only one user per cell operates on a particular frequency at a time. This chapter will present the analysis used to find the multiuser interference terms due to the first-tier co-channel cells in the different microzoning layouts. Distances will be given in term of R_z, the zone radius.

As will be demonstrated in the numerical analysis chapter, the inclusion of the second-tier co-channel interfering cells has a very minor effect on the overall S/N ratio. This result, coupled with the added complexity of the microzoning technique, justifies the omission of second-tier co-channel interference from the analysis in this chapter.

1. Lee's Method for One-cell per Cluster Microzoning

The first layout is a one-cell per cluster microzoning system as seen in Figure 3.3.

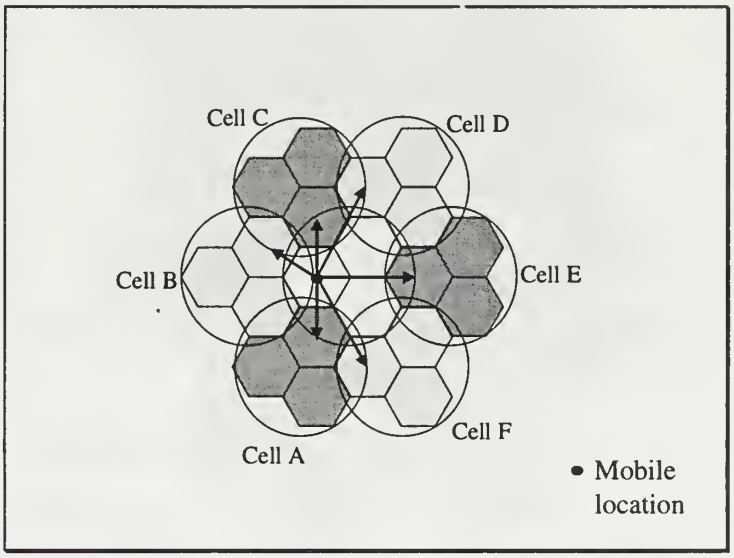

Figure 3.3: One-cell per Cluster Lee Microzoning Method.

The center cell is the original, or reference cell. The mobile user is located in the left-most zone of the reference cell. Because this is a one-cell per cluster system, all the cells use the same set of frequencies, and hence, are all co-channel interferers with one another. The distances from the mobile unit to the center of the nearest zone of cells A,

B, and C are equal, with a value of $\sqrt{3}R_z$. The distances from the mobile unit to the center of the nearest zone of cells D, E, and F are also equal, with a value of $3R_z$. The resulting first-tier co-channel interference term at this location is given by

$$\left(\frac{S}{I}\right)_{CCI-1}^{-1} = \left[\frac{\left(\sqrt{3}R_z\right)^{-n_A} + \left(\sqrt{3}R_z\right)^{-n_B} + \left(\sqrt{3}R_z\right)^{-n_C} + \left(3R_z\right)^{-n_D} + \left(3R_z\right)^{-n_E} + \left(3R_z\right)^{-n_F}}{R_z^{-n_0}}\right] \tag{3.1}$$

The co-channel distances presented above are raised to their respective path loss exponents n_A through n_F. The path loss exponent for the reference cell is n_0.

2. Lee's Method for Three-cell per Cluster Microzoning

The architecture and measured distances for the three-cell per cluster microzoning system using Lee's method can be seen in Figure 3.4.

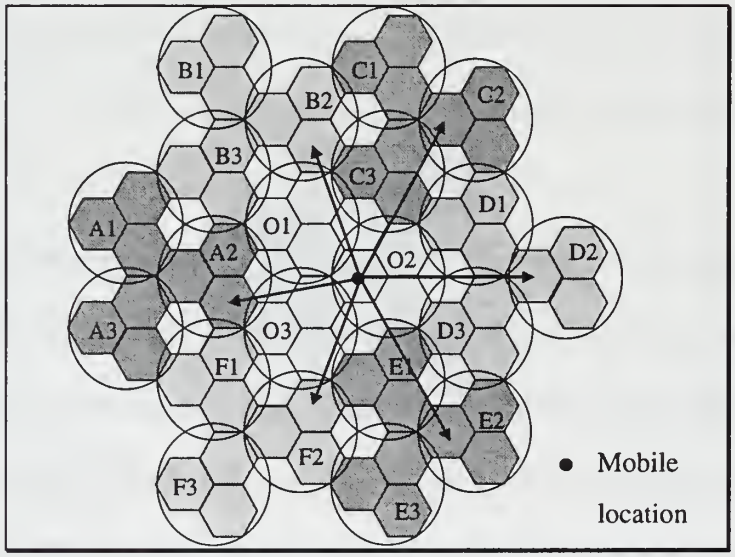

Figure 3.4: Three-cell per Cluster Lee Microzoning Method.

Here the mobile user is located in the left-most zone of cell two of the reference cluster. The co-channel interfering cells are A2, B2, C2, D2, E2, and F2. The distances from the mobile unit to the center of the nearest zone of cells A2, B2, and F2 are equal, with a value of $\sqrt{21}R_z$. The distances from the mobile unit to the center of the nearest

zone of cells C2, D2, and E2 are also equal, with a value of $6R_z$. The resulting first-tier interference term at this location is given by

$$\left(\frac{S}{I}\right)^{-1}_{CCI-1} = \left[\frac{\left(\sqrt{21}R_z\right)^{-n_a} + \left(\sqrt{21}R_z\right)^{-n_B} + \left(6R_z\right)^{-n_C} + \left(6R_z\right)^{-n_D} + \left(6R_z\right)^{-n_E} + \left(\sqrt{21}R_z\right)^{-n_F}}{R_z^{-n_0}}\right] \tag{3.2}$$

3. Lee's Method for Seven-cell per Cluster Microzoning

The layout and measured distances for the seven-cell per cluster microzoning system using Lee's method are shown in Figure 3.5.

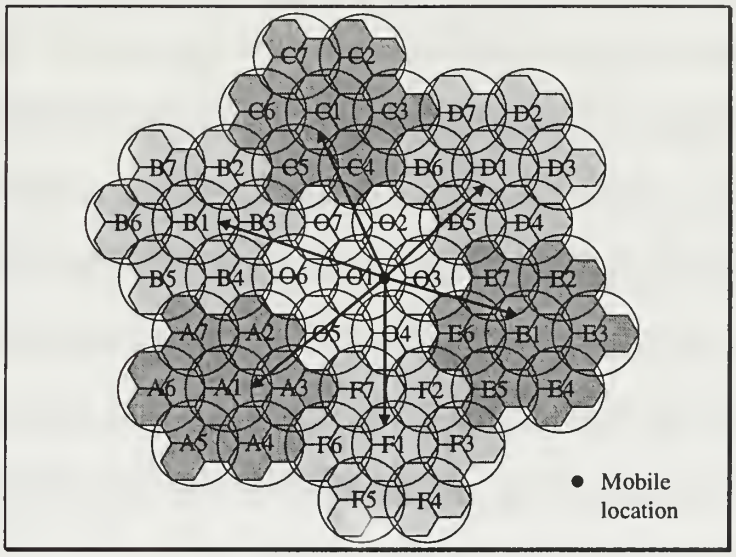

Figure 3.5: Seven-cell per Cluster Lee Microzoning Method.

Here the mobile unit is located in the right-most zone of cell one of the reference, or center, cluster. The co-channel interfering cells are A1, B1, C1, D1, E1, and F1. The distances from the mobile unit to the center of the nearest zone of cells A1 and B1 are equal with a value of $\sqrt{63}R_z$. The distances to the center of the nearest zone of cells D1 and E1 are equal with a value of $\sqrt{39}R_z$. The distance to the center of the nearest zone of

cell C1 is $\sqrt{57}R_z$, while the distance to the center of the nearest zone of cell F1 is $\sqrt{48}R_z$. These values yield a first-tier interference term at this location of

$$\left(\frac{S}{I}\right)^{-1}_{CCI-1} = \left[\frac{\left(\sqrt{63}R_z\right)^{-n_A} + \left(\sqrt{63}R_z\right)^{-n_B} + \left(\sqrt{57}R_z\right)^{-n_C} + \left(\sqrt{39}R_z\right)^{-n_D} + \left(\sqrt{39}R_z\right)^{-n_E} + \left(\sqrt{48}R_z\right)^{-n_F}}{R_z^{-n_0}}\right] \quad (3.3)$$

C. MAYER'S MICROZONING METHOD (VERSION ONE)

As mentioned earlier in this chapter, Lee's microzoning method does not take into account the position and directivity of the zone transmitters. In the remaining sections of this chapter, Mayer's distance measurement method for microzoning, which consider the location and orientation of the three individual zone transmitters, will be presented.

Taking zone antenna positions into account, we find that several zones (one to two per cell, depending on the geometry) will not create interference at the mobile due to the direction of their antenna radiation pattern. As a result, the distances between zones of co-channel cells are farther apart than those used in the analysis by Lee, as seen in Figure 3.6. This, in turn, helps improve the signal-to-noise plus interference ratio.

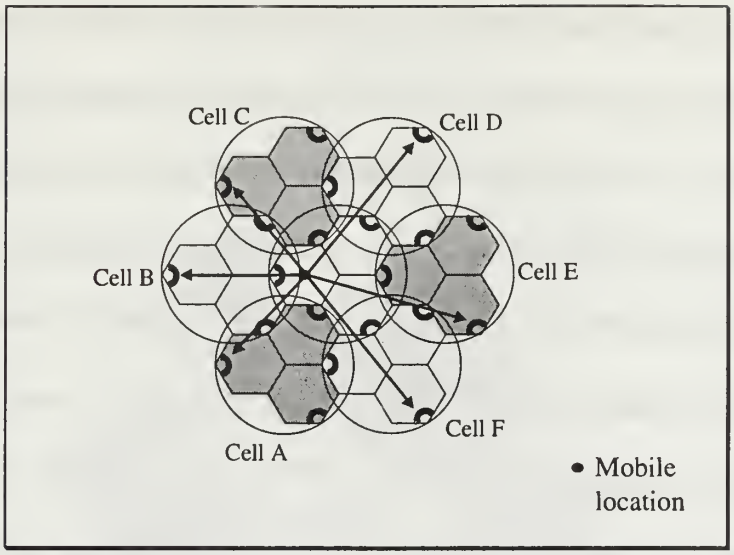

Figure 3.6: Mayer's Microzoning Method (Version One) for a One-cell per Cluster System.

In this figure, the zone transmitters are designated by black semi-circles. Each zone transmitter lies on the outer edge of its zone, and hence, the outer edge of its cell as well. The zone antennas radiate back toward the center of the cell with a 120° radiation pattern. The difference between Lee's method and this method can easily be seen by examining the co-channel distance from the mobile unit to co-channel cell A. Lee's method uses the distance from the mobile unit to the center of the nearest zone in cell/cluster A. This is the center of the top-most zone of cell A. However, the antenna for that zone is radiating away from the mobile user, and hence is not a source of interference to the mobile. Instead, the left-most and bottom zones of cell A are the only zones that generate interference to the mobile user, and hence the only zones that should be considered for the interference distance measurement. Since the distance from the mobile to the transmitter of the left-most zone of cell A is $\sqrt{13}R_z$ and the distance from the mobile to the transmitter of the bottom zone of cell A is $\sqrt{19}R_z$, Mayer's method chooses the distance to left-most zone of cell A as the interference distance. Again, this

decision is based upon choosing the transmitter closest to the mobile of those eligible to create interference with the mobile, since only one zone transmitter of a cell is active on a particular frequency at a time in the narrowband FDMA system. Recall Lee's distance measurement method for the one-cell per cluster architecture resulted in choosing an ineligible zone transmitter (the top zone) in cell A, which yielded an interference distance of $\sqrt{3}R_z$. All other things being equal, the more accurate distance measurements utilized by Mayer's microzoning method (version one) at least equal, although almost always increase, the interference distance for each co-channel cell. This, in turn, lowers the co-channel interference term.

1. Mayer's Method for One-cell per Cluster Microzoning (Version One)

The one-cell per cluster layout using Mayer's method (version one) is shown in Figure 3.6 in the previous section. The distances from the mobile unit to the appropriate zones of co-channel cells A and C are equal, with a value of $\sqrt{13}R_z$. The distances to the appropriate zones of co-channel cells D and F are equal with a value of $\sqrt{31}R_z$. Finally the distance to the appropriate zone of co-channel B is $4R_z$, and the distance to the appropriate zone of co-channel E is $\sqrt{28}R_z$. These values produce an expression for the first-tier co-channel interference term as follows

$$\left(\frac{S}{I}\right)^{-1}_{CCI-1} = \left[\frac{\left(\sqrt{13}R_z\right)^{-n_a} + \left(4R_z\right)^{-n_B} + \left(\sqrt{13}R_z\right)^{-n_C} + \left(\sqrt{31}R_z\right)^{-n_D} + \left(\sqrt{28}R_z\right)^{-n_E} + \left(\sqrt{31}R_z\right)^{-n_F}}{R_z^{-n_0}}\right] \tag{3.4}$$

This can be compared to Lee's result, given by equation 3.1.

2. Mayer's Method for Three-cell per Cluster Microzoning (Version One)

The architecture and measured distances for the three-cell per cluster microzoning system using Mayer's method (version one) are shown in Figure 3.7.

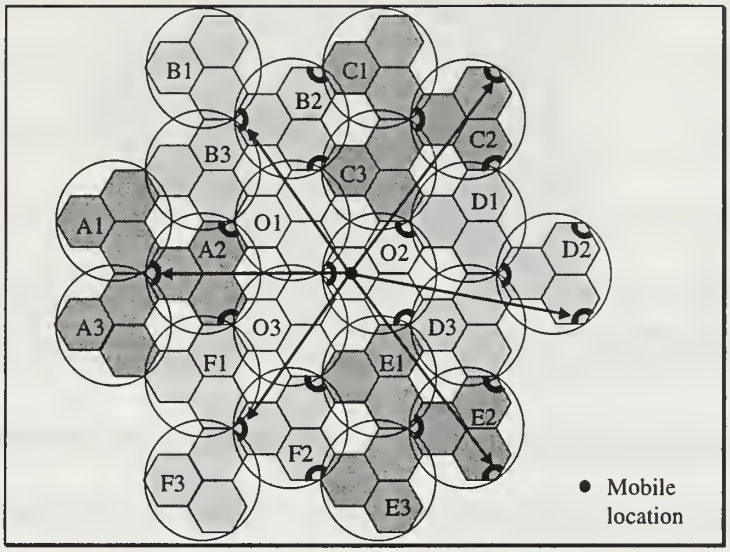

Figure 3.7: Mayer's Microzoning Method (Version One) for a Three-cell per Cluster System.

The mobile unit is located in the left-most zone of cell two of the reference, or center, cluster. The co-channel interfering cells are A2, B2, C2, D2, E2, and F2. The interference distances from the mobile unit to the transmitter of the appropriate zones of each of the co-channel cells are $7R_z$, $\sqrt{43}R_z$, $\sqrt{73}R_z$, $\sqrt{67}R_z$, $\sqrt{73}R_z$, and $\sqrt{43}R_z$, respectively. The resulting first-tier interference term is given by

$$\left(\frac{S}{I}\right)^{-1}_{1CI} = \left[\frac{(7R_z)^{-n_A} + (\sqrt{43}R_z)^{-n_B} + (\sqrt{73}R_z)^{-n_C} + (\sqrt{67}R_z)^{-n_D} + (\sqrt{73}R_z)^{-n_E} + (\sqrt{43}R_z)^{-n_F}}{R_z^{-n_0}}\right] \quad (3.5)$$

This can be compared with Lee's result, given by equation 3.2.

3. Mayer's Method for Seven-cell per Cluster Microzoning (Version One)

Figure 3.8 shows the layout and distance measurements for the seven-cell per cluster system using Mayer's microzoning method (version one).

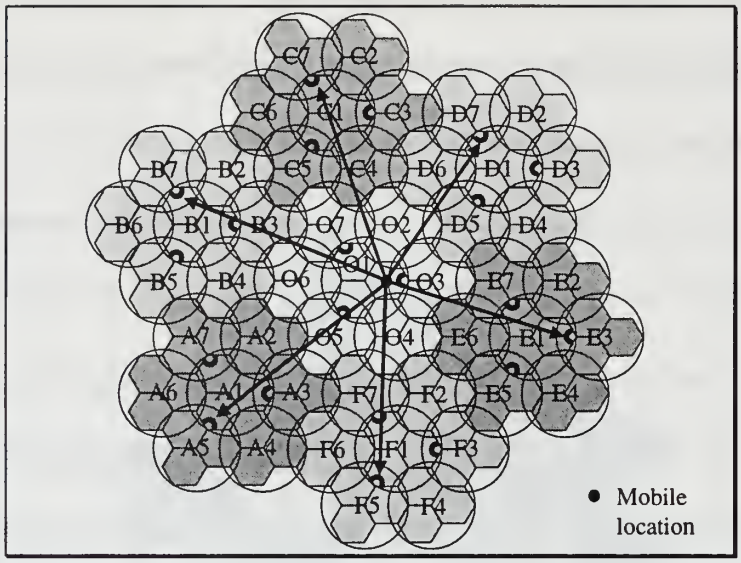

Figure 3.8: Mayer's Microzoning Method (Version One) for a Seven-cell per Cluster System.

In this figure, the mobile is located in the right-most zone of cell one of the reference cluster. The co-channel interfering cells are A1, B1, C1, D1, E1, and F1. The interference distances from the mobile unit to the transmitter of the appropriate zones of each of the co-channel cells are $\sqrt{112}R_z$, $\sqrt{109}R_z$, $\sqrt{103}R_z$, $\sqrt{64}R_z$, $\sqrt{79}R_z$, and $\sqrt{91}R_z$, respectively. The resulting first-tier interference term is given by

$$\left(\frac{S}{I}\right)_{CCI-1}^{-1} = \left[\frac{\left(\sqrt{112}R_z\right)^{-n_A} + \left(\sqrt{109}R_z\right)^{-n_B} + \left(\sqrt{103}R_z\right)^{-n_C}}{R_z^{-n_0}} + \frac{\left(\sqrt{64}R_z\right)^{-n_D} + \left(\sqrt{79}R_z\right)^{-n_E} + \left(\sqrt{91}R_z\right)^{-n_F}}{R_z^{-n_0}}\right] \tag{3.6}$$

This can be compared with Lee's result, given by equation 3.3.

D. MAYER'S MICROZONING METHOD (VERSION TWO)

For both Lee's method and Mayer's method (version one) of microzoning, the mobile location is considered to be one zone radius away from the desired zone

transmitter. In other words, the mobile is depicted as being in the center of its parent zone. Perhaps the reasoning behind this choice is that the antenna radiation patterns of the three zone transmitters may overlap to some extent. Therefore, a mobile located at a distance of two times the zone radius from one of the zone transmitters will likely be at a closer distance to another zone transmitter. While this may be more accurate in practice, it does not represent the absolute worst case scenario. The worst case is represented when the mobile unit lies in the center of the cell, equally far from each zone transmitter. This occurs when the distance from the desired zone transmitter to mobile is two times the radius of the zone. In the spirit of finding an upper bound on the interference level, a combination of the more accurate co-channel distances, explained earlier in Mayer's microzoning method (version one), paired with the conservative desired zone transmitter to mobile distance of two times the zone radius, is used. The distance measurements of a one-cell per cluster layout for this conservative version of Mayer's microzoning, which will be called Mayer's method (version two), is shown in Figure 3.9.

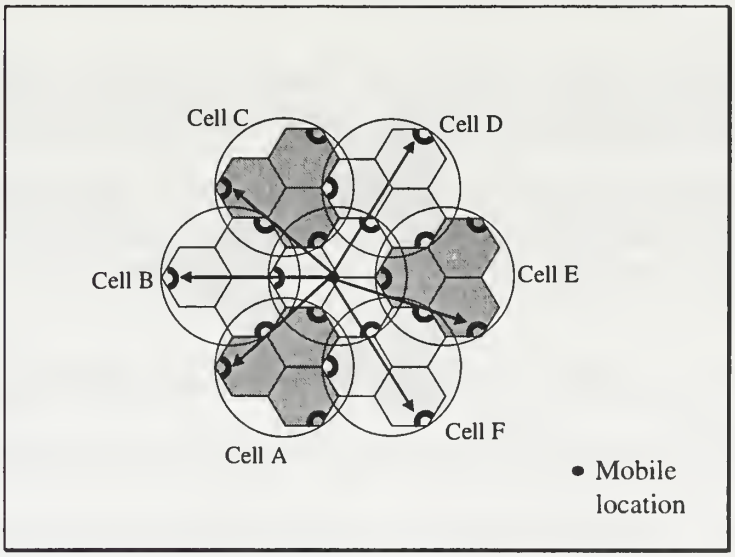

Figure 3.9: Mayer's Microzoning Method (Version Two) for a One-cell per Cluster System.

1. Mayer's Method for One-cell per Cluster Microzoning (Version Two)

This section will present the analysis and derivation of the co-channel interference term for the one-cell per cluster layout using Mayer's method (version two). Figure 3.9 in the previous section depicts this architecture. For the worst case scenario, the mobile unit is considered to be in the center of its cell, equally far from all zone transmitters. In the figure, the mobile unit is shown just to the left of the center point of the cell so it falls under the control of the left-most zone of the reference, or center cell. For analysis purposes, two times the zone radius is used as the zone transmitter to mobile distance. The interference distances from the mobile unit to the transmitter of the appropriate zones of each of the co-channel cells, A, B, C, D, E, and F, are $\sqrt{19}R_z$, $5R_z$, $\sqrt{19}R_z$, $5R_z$, $\sqrt{19}R_z$, and $5R_z$, respectively. The resulting first-tier interference term is given by

$$\left(\frac{S}{I}\right)^{-1}_{CCI-1} = \left[\frac{\left(\sqrt{19}R_z\right)^{-n_A} + \left(5R_z\right)^{-n_B} + \left(\sqrt{19}R_z\right)^{-n_C} + \left(5R_z\right)^{-n_D} + \left(\sqrt{19}R_z\right)^{-n_E} + \left(5R_z\right)^{-n_F}}{\left(2R_z\right)^{-n_0}}\right] \tag{3.7}$$

This can be compared with the result for Mayer's method (version one), given by equation 3.4.

2. Mayer's Method for Three-cell per Cluster Microzoning (Version Two)

The architecture and measured distances for the three-cell per cluster microzoning system using Mayer's method (version two) are shown in Figure 3.10.

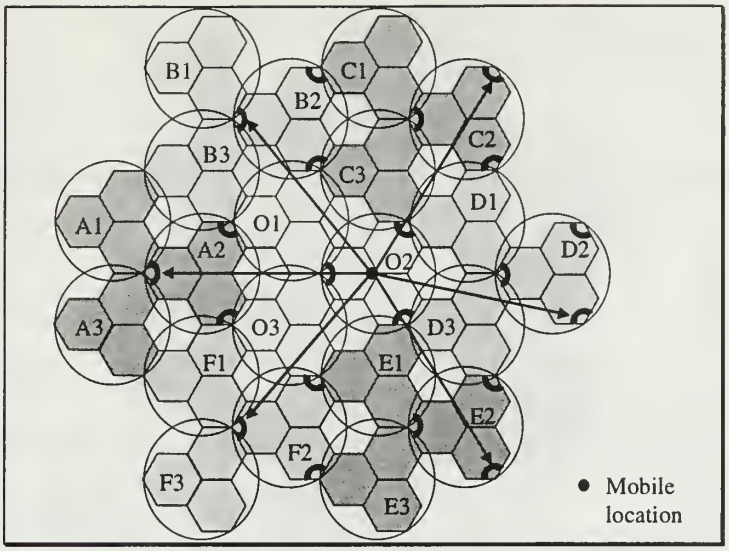

Figure 3.10: Mayer's Microzoning Method (Version Two) for a Three-cell per Cluster System.

In the figure, the mobile unit is shown just to the left of the center of cell two of the reference cluster, so it falls under the control of the left-most zone of cell O2. The distances from the mobile unit to the appropriate zone transmitters of co-channel interfering cells A2, C2, and E2 are equal with a value of $8R_z$, while the distances to B2, D2, and F2 are equal with a value of $\sqrt{52}R_z$. This yields a co-channel interference term denoted by

$$\left(\frac{S}{I}\right)_{CCI-1}^{-1} = \left[\frac{(8R_z)^{-n_A} + (\sqrt{52}R_z)^{-n_B} + (8R_z)^{-n_C} + (\sqrt{52}R_z)^{-n_D} + (8R_z)^{-n_E} + (\sqrt{52}R_z)^{-n_F}}{(2R_z)^{-n_0}}\right] \quad (3.8)$$

This can be compared with the result for Mayer's method (version one), given by equation 3.5.

3. Mayer's Method for Seven-cell per Cluster Microzoning (Version Two)

The architecture and measured distances for the seven-cell per cluster microzoning system using Mayer's method (version two) are shown in Figure 3.11.

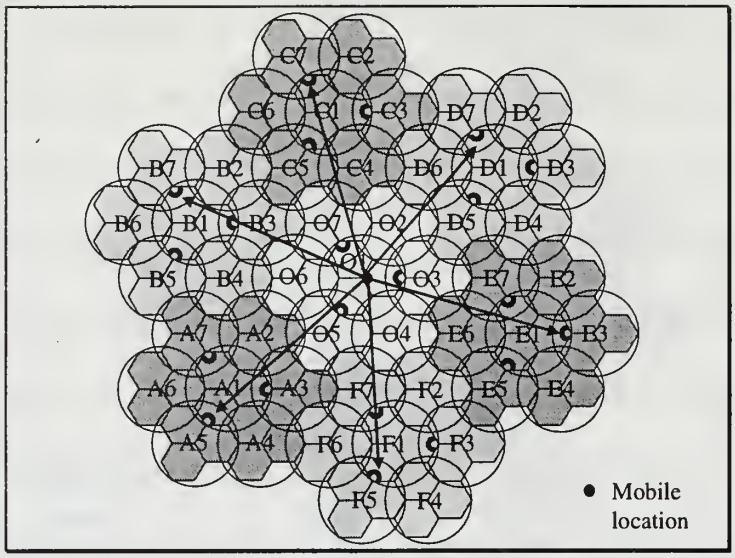

Figure 3.11: Mayer's Microzoning Method (Version Two) for a Seven-cell per Cluster System.

In the figure, the mobile unit is shown just to the right of the center of cell one of the reference cluster, falling under the control of the right-most zone of cell O1. The distances from the mobile unit to the appropriate zone transmitters of co-channel interfering cells A1, C1, and E1 are equal with a value of $\sqrt{97}R_z$. The distances to B1, and F1 are equal with a value of $\sqrt{91}R_z$, while the distance to D1 is $\sqrt{73}R_z$. Of note, the geometry of the seven-cell per cluster layout is such that the right-most zone of cell D1 is the only zone that generates interference into the reference zone regardless of the mobile's placement. Because we are looking at the absolute worst case scenario, though, the top-most zone is chosen since it is a closer distance. However, due to its transmitter's orientation, it would not be able to generate interference as received by the mobile when the mobile is at the worst case location as shown in Figure 3.11. As such, the conservative co-channel interference term for this architecture is denoted by

$$\left(\frac{S}{I}\right)^{-1}_{CCI-1} = \left[\frac{\left(\sqrt{97}R_z\right)^{-n_a} + \left(\sqrt{91}R_z\right)^{-n_b} + \left(\sqrt{97}R_z\right)^{-n_c}}{\left(2R_z\right)^{-n_0}} + \right.$$

$$\left[\frac{\left(\sqrt{73}R_Z\right)^{-n_D}+\left(\sqrt{97}R_Z\right)^{-n_E}+\left(\sqrt{91}R_Z\right)^{-n_F}}{\left(2R_Z\right)^{-n_0}}\right] \tag{3.9}$$

This can be compared with the result from Mayer's method (version one), given by equation 3.6.

E. SUMMARY

A quick reference for finding the first-tier co-channel interference equations for each of the microzoning architectures is given in Table 3.1.

	One-cell per cluster	Three-cell per cluster	Seven-cell per cluster
Lee's method	Equation 3.1	Equation 3.2	Equation 3.3
Mayer's method Version 1	Equation 3.4	Equation 3.5	Equation 3.6
Mayer's method Version 2	Equation 3.7	Equation 3.8	Equation 3.9

Table 3.1: Equation Reference for Chapter III Architectures

Because of the greater distance between the mobile user and the desired zone transmitter associated with Mayer's microzoning method (version two), one would expect its overall co-channel interference to be greater than both Lee's method and Mayer's previously described microzoning method (version one). As expected, Mayer's version one method always produces less interference than Mayer's version two method. As compared with Lee, his erroneous method yields less interference for the three-cell per cluster and seven-cell per cluster layouts than Mayer's version two method does, however this is not the case with the one-cell per cluster design. Mayer's conservative version two method still generates less interference than Lee's erroneous method in the one-cell per cluster layout. Hence, for the one-cell per cluster design, Lee's results are

too conservative, while for the three-cell and seven-cell per cluster designs, Lee's results are optimistic. These comments will be quantified in the numerical analysis chapter.

A direct comparison between Lee's method and Mayer's method (version one) can be easily performed since they both use the same mobile unit placement. However, for a truly accurate representation of which method yields the lowest interference in a worst case situation, Lee's method should be modified to account for the mobile's worst case placement which is twice the zone radius away from the desired zone transmitter. His analysis currently uses only half the worst case distance from the mobile unit to the desired zone transmitter. Once his mobile unit correctly depicts the worst case placement, then an apples-to-apples comparison between Mayer's method (version two) and his method can be performed.

With the signal-to-interference plus noise expressions developed for all combinations of the one-cell, three-cell, and seven-cell per cluster architectures for Lee's method, Mayer's method (version one), and Mayer's method (version two), performance can be evaluated. This will be done in the numerical analysis chapter using specific values for path loss exponents, cell radius, signal bit energy to noise ratio (E_b/N_0), and processing gain.

In the next chapter, Mayer's method versions one and two will be extended to the analysis of microzoning in wideband CDMA systems.

IV. THE WIDEBAND MICROZONING CONCEPT

A. DIFFERENCES BETWEEN NARROWBAND AND WIDEBAND MICROZONING

In Chapter III, the analysis of microzoning in a narrowband FDMA system were presented. Because only one zone transmitter transmits to a specific user on a specific frequency at a time, only one zone of each co-channel cell creates interference as received by the mobile unit. When extending this concept to a CDMA system, all of the zones of the co-channel cells can potentially create interference provided that the directionality of their antennas allows them to radiate into the desired zone. As such, there will be more zones generating interference as will be shown in this chapter.

The difference in trunking efficiency between sectoring and microzoning in the framework of a CDMA system is similar to that in the FDMA system. Referring back to microzoning in an FDMA environment, the mobile can stay on the same assigned frequency when it moves from zone to zone within a cell. Control of that frequency is just switched to the appropriate zone, preserving the trunking efficiency of the system. Sectoring in an FDMA environment requires the base station to switch to a new frequency specifically assigned to a particular sector when the mobile moves into that sector from another sector in the cell. Here the trunking efficiency is divided by the number of sectors per cell, hence the advantage of microzoning over sectoring.

In the CDMA case, sectoring requires the base station to switch to a unique code specifically assigned to a particular sector when the mobile travels into that sector from another sector within the cell. Microzoning in the CDMA context allows for the mobile to stay on the same assigned code when it moves from zone to zone within a cell. Control of that code is just switched to the appropriate zone. In this fashion, bandwidth

limitations allow a maximum of N users per cell for microzoning, as opposed to N/3 for 120° sectoring, and N/6 for 60° sectoring. Recall, N is the number of unique codes available for individual users on the forward channel. As a result, microzoning is the best candidate for the CDMA system, even after the additional interfering zones have been included in the co-channel interference equations. Additionally, the same reduction in system overhead associated with microzoning's soft hand-off is still an advantage within the framework of a CDMA system.

Mayer's methods versions one and two will be modified to measure the co-channel interference of a CDMA system in one-cell, three-cell, and seven-cell per cluster layouts in this chapter. Equation 2.1 will be used for finding the signal-to-interference plus noise ratio for all architectures presented in this chapter. The AWGN term will be the same as in the previous chapters, and the multiuser interference within the reference cell will be zero due to the orthogonal spreading codes. Distances will be given in terms of R_z, the zone radius. Again, due to the minor effect of the second-tier interferers, only first-tier interfering cells will be considered as in the narrowband microzoning case.

B. MAYER'S MICROZONING METHOD (VERSION ONE)

As mentioned earlier in this chapter, more than one zone of a co-channel cell may be transmitting at a time on the same frequency band in a CDMA system. As a result, more than one zone per co-channel cell may produce interference as received by the mobile unit. Whether or not it does, and the extent to which it does, depends upon the transmitter's location. In this chapter, the additional interference will be identified, analyzed, and included in the S/N equations.

1. Mayer's Method for One-cell per Cluster Microzoning (Version One)

In Figure 4.1, the solid lines represent the interference generated into the desired zone of the reference cell in the narrowband FDMA system. In a CDMA system, additional interference is generated by both remaining zones of cell B, the top-most zone of cell C, the top-most zone of cell E, and the bottom-most zone of cell A. The distances from the mobile unit to the additional interfering zone transmitters are noted by the dashed lines.

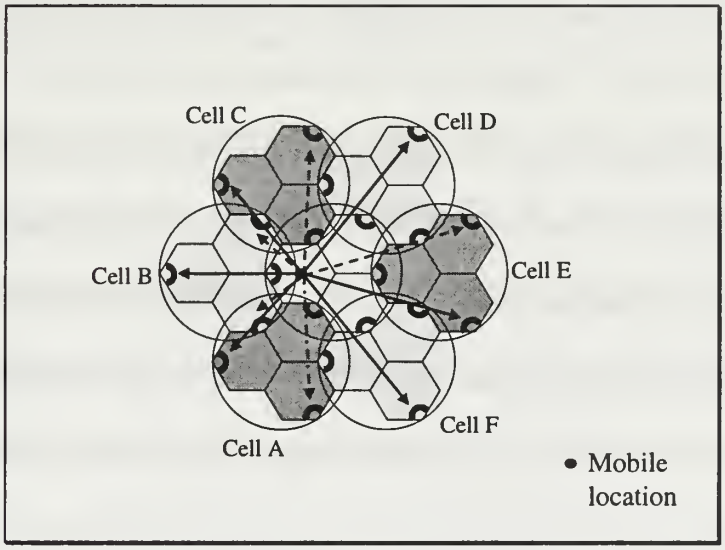

Figure 4.1: Mayer's Microzoning Method (Version One) for a One-cell per Cluster System.

The distances from the mobile unit to the additional interfering zones of co-channel cells A and C are equal, with a value of $\sqrt{19}R_z$. The distance to the additional interfering zone of co-channel cell E is $\sqrt{28}R_z$. Finally the distances to the two additional interfering zones of co-channel B are equal with a value of $2R_z$. Using these values, we obtain the first-tier co-channel interference term as follows

$$\left(\frac{S}{I}\right)^{-1}_{CCI-1} = \frac{2}{3N}\left[\frac{K_{A1}\left(\sqrt{13}R_z\right)^{-n_{A1}} + K_{B1}\left(4R_z\right)^{-n_{B1}} + K_{C1}\left(\sqrt{13}R_z\right)^{-n_{C1}}}{R_z^{-n_0}} + \right.$$

$$\frac{K_{D1}\left(\sqrt{31}R_z\right)^{-n_{D1}}+K_{E1}\left(\sqrt{28}R_z\right)^{-n_{E1}}+K_{F1}\left(\sqrt{31}R_z\right)^{-n_{F1}}+K_{A2}\left(\sqrt{19}R_z\right)^{-n_{A2}}}{R_z^{-n_0}}+$$

$$\left.\frac{K_{B2}\left(2R_z\right)^{-n_{B2}}+K_{B3}\left(2R_z\right)^{-n_{B3}}+K_{C2}\left(\sqrt{19}R_z\right)^{-n_{C2}}+K_{E2}\left(\sqrt{28}R_z\right)^{-n_{E2}}}{R_z^{-n_0}}\right] \quad (4.1)$$

In equation 4.1, the subscripts K_{A1} through K_{F1} represent the number of users in the original interfering zones of the co-channel cells as presented in Chapter III. K_{A2}, K_{C2}, and K_{E2} represent the number of users per zone of the additional interfering zones of cells A, C, and E, respectively. Finally, K_{B2} and K_{B3} represent the number of users each in the top-most and bottom-most zones of cell B, which present potential additional interference. These two zones are included to represent an upper bound on interference. In reality, if the two additional zones of cell B are generating interference into the reference zone of the desired cell as received by the mobile, the mobile unit is closer to the transmitter than the previously established worst-case location for Mayer's method (version one).

2. Mayer's Method for Three-cell per Cluster Microzoning (Version One)

The architecture and measured distances for the three-cell per cluster microzoning system using Mayer's method (version one) are shown in Figure 4.2.

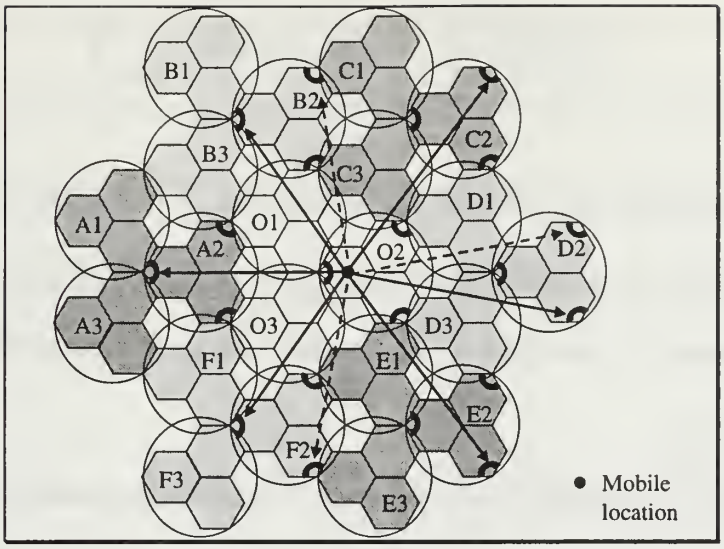

Figure 4.2: Mayer's Microzoning Method (Version One) for a Three-cell per Cluster System.

The mobile unit is located in the left-most zone of cell two of the reference, or center, cluster. The co-channel interfering cells are A2, B2, C2, D2, E2, and F2. The interference distances from the mobile unit to the transmitter of the original interfering zones of each of the co-channel cells are $7R_z$, $\sqrt{43}R_z$, $\sqrt{73}R_z$, $\sqrt{67}R_z$, $\sqrt{73}R_z$, and $\sqrt{43}R_z$, respectively. The distances from the mobile unit to the transmitter of the additional interfering zones of cell B2, D2, and F2 are denoted by the dashed lines. They are $\sqrt{49}R_z$, $\sqrt{67}R_z$, and $\sqrt{49}R_z$, respectively. The resulting first-tier interference term is given by

$$\left(\frac{S}{I}\right)^{-1}_{CCI-1} = \frac{2}{3N}\left[\frac{K_{A1}\left(7R_z\right)^{-n_{A1}} + K_{B1}\left(\sqrt{43}R_z\right)^{-n_{B1}} + K_{C1}\left(\sqrt{73}R_z\right)^{-n_{C1}}}{R_z{}^{-n_0}} + \right.$$

$$\left.\frac{K_{D1}\left(\sqrt{67}R_z\right)^{-n_{D1}} + K_{E1}\left(\sqrt{73}R_z\right)^{-n_{E1}} + K_{F1}\left(\sqrt{43}R_z\right)^{-n_{F1}} + K_{B2}\left(\sqrt{49}R_z\right)^{-n_{B2}}}{R_z{}^{-n_0}} + \right.$$

$$\frac{K_{D2}\left(\sqrt{67}R_z\right)^{-n_{D2}} + K_{F2}\left(\sqrt{49}R_z\right)^{-n_{F2}}}{R_z^{-n_0}}\Bigg] \tag{4.2}$$

Here again, the subscripts K_{A1} through K_{F1} represent the number of users in the original interfering zones of the co-channel cells as presented in Chapter III. K_{B2}, K_{D2}, and K_{F2} represent the number of users per zone of the additional interfering zones of cells B2, D2, and F2, respectively.

3. Mayer's Method for Seven-cell per Cluster Microzoning (Version One)

Figure 4.3 shows the layout and distance measurements for the seven-cell per cluster system using Mayer's microzoning method (version one).

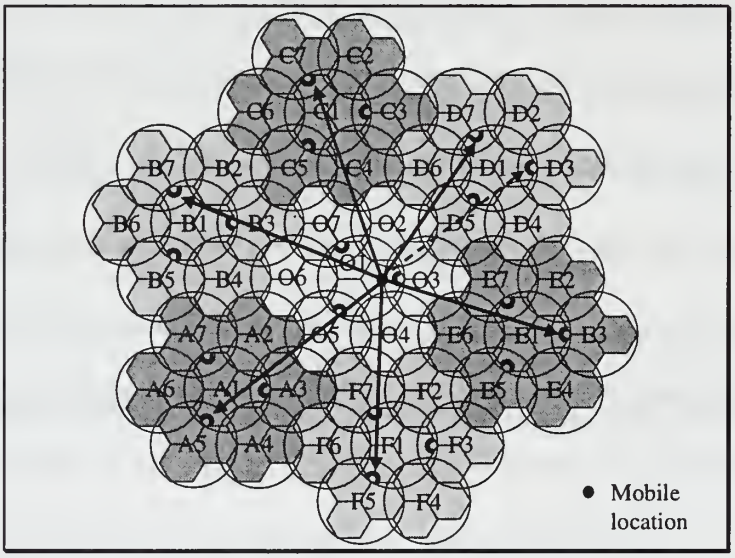

Figure 4.3: Mayer's Microzoning Method (Version One) for a Seven-cell per Cluster System.

In this figure, the mobile is located in the right-most zone of cell one of the reference cluster. The co-channel interfering cells are A1, B1, C1, D1, E1, and F1. The interference distances from the mobile unit to the transmitter of the original interfering zones of each of the co-channel cells are $\sqrt{112}R_z$, $\sqrt{109}R_z$, $\sqrt{103}R_z$, $\sqrt{64}R_z$, $\sqrt{79}R_z$, and $\sqrt{91}R_z$, respectively. In this architecture, cell D1 is the only cell that has an

additional zone that could introduce interference into the reference zone of the desired cell. The distance from that zone, the right-most zone of cell D1, is $\sqrt{76}R_z$ and is denoted with a dashed line. The resulting first-tier interference term is given by

$$\left(\frac{S}{I}\right)^{-1}_{CCI-1} = \frac{2}{3N}\left[\frac{K_{A1}\left(\sqrt{112}R_z\right)^{-n_{A1}} + K_{B1}\left(\sqrt{109}R_z\right)^{-n_{B1}} + K_{C1}\left(\sqrt{103}R_z\right)^{-n_{C1}}}{R_z^{-n_0}} + \right.$$

$$\left. \frac{K_{D1}\left(\sqrt{64}R_z\right)^{-n_{D1}} + K_{E1}\left(\sqrt{79}R_z\right)^{-n_{E1}} + K_{F1}\left(\sqrt{91}R_z\right)^{-n_{F1}} + K_{D2}\left(\sqrt{76}R_z\right)^{-n_{D2}}}{R_z^{-n_0}}\right] \quad (4.3)$$

Here the subscripts K_{A1} through K_{F1} represent the number of users in the original interfering zones of the co-channel cells as presented in Chapter III. K_{D2} represents the number of users in the additional interfering zone of cell D1.

C. MAYER'S MICROZONING METHOD (VERSION TWO)

Now we will extend Mayer's method (version two) to handle the co-channel interference analysis of a CDMA system. Recall in this version, the worst case is represented when the mobile unit lies in the center of the cell, equally far from each zone transmitter. This occurs when the distance from the desired zone transmitter to mobile is two times the radius of the zone. In the spirit of finding an upper bound on the interference level, this conservative zone transmitter to mobile distance of two times the zone radius is used.

1. Mayer's Method for One-cell per Cluster Microzoning (Version Two)

For this architecture, the mobile unit is shown just to the left of the center point of the cell so it falls under the control of the left-most zone of the reference, or center cell in

Figure 4.4. For analysis purposes, two times the zone radius is used as the zone transmitter to mobile distance.

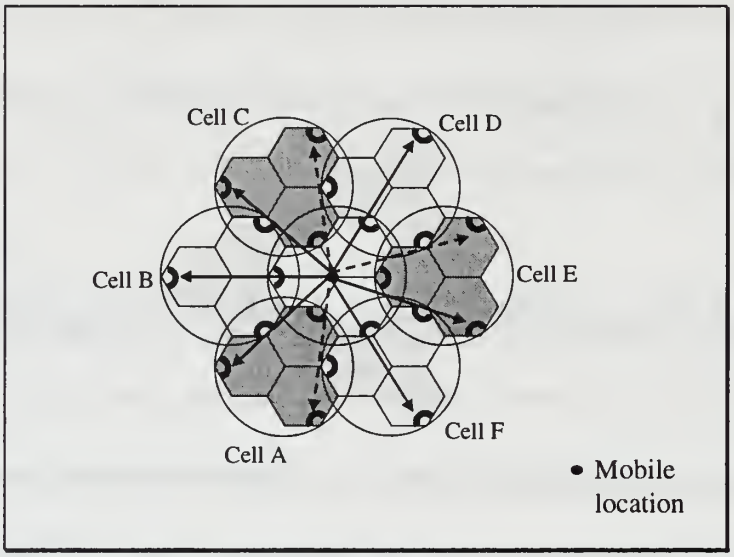

Figure 4.4: Mayer's Microzoning Method (Version Two) for a One-cell per Cluster System.

The interference distances from the mobile unit to the transmitter of the original interfering zones of each of the co-channel cells, A, B, C, D, E, and F, are $\sqrt{19}R_z$, $5R_z$, $\sqrt{19}R_z$, $5R_z$, $\sqrt{19}R_z$, and $5R_z$, respectively. The distances from the mobile unit to the additional interfering zones of co-channel A, C, and E are equal with a value of $\sqrt{19}R_z$ and shown in Figure 4.4 with dashed lines. The resulting first-tier interference term is given by

$$\left(\frac{S}{I}\right)^{-1}_{CCI-1} = \frac{2}{3N}\left[\frac{K_{A1}\left(\sqrt{19}R_z\right)^{-n_{A1}} + K_{B1}\left(5R_z\right)^{-n_{B1}} + K_{C1}\left(\sqrt{19}R_z\right)^{-n_{C1}}}{\left(2R_z\right)^{-n_0}} + \right.$$

$$\left.\frac{K_{D1}\left(5R_z\right)^{-n_{D1}} + K_{E1}\left(\sqrt{19}R_z\right)^{-n_{E1}} + K_{F1}\left(5R_z\right)^{-n_{F1}} + K_{A2}\left(\sqrt{19}R_z\right)^{-n_{A2}}}{\left(2R_z\right)^{-n_0}} + \right.$$

$$\frac{K_{C2}\left(\sqrt{19}R_z\right)^{-n_{C2}} + K_{E2}\left(\sqrt{19}R_z\right)^{-n_{E2}}}{\left(2R_z\right)^{-n_0}}\Bigg] \tag{4.4}$$

In equation 4.4, the subscripts K_{A1} through K_{F1} represent the number of users in the original interfering zones of the co-channel cells as presented in Chapter III. K_{A2}, K_{C2}, and K_{E2} represent the number of users per zone of the additional interfering zones of cells A, C, and E, respectively.

2. Mayer's Method for Three-cell per Cluster Microzoning (Version Two)

The architecture and measured distances for the three-cell per cluster microzoning system using Mayer's method (version two) are shown in Figure 4.5.

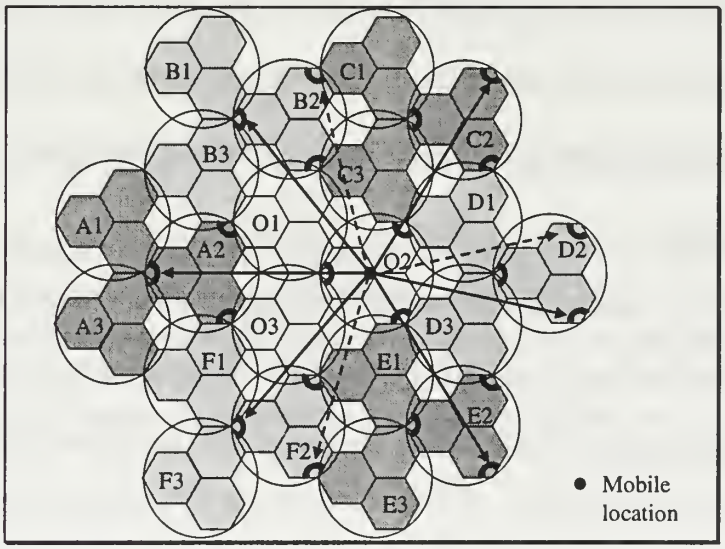

Figure 4.5: Mayer's Microzoning Method (Version Two) for a Three-cell per Cluster System.

In the figure, the mobile unit is shown just to the left of the center of cell two of the reference cluster, so it falls under the control of the left-most zone of cell O2. The distances from the mobile unit to the original zone transmitters of co-channel interfering cells A2, C2, and E2 are equal with a value of $8R_z$, while the distances to B2, D2, and F2 are equal with a value of $\sqrt{52}R_z$. The distances from the mobile unit to the transmitter of

the additional interfering zones of cell B2, D2, and F2 are denoted by the dashed lines. They are all equal to $\sqrt{52}R_z$. This yields a co-channel interference term denoted by

$$\left(\frac{S}{I}\right)^{-1}_{CCI-1} = \frac{2}{3N}\left[\frac{K_{A1}(8R_z)^{-n_{A1}} + K_{B1}(\sqrt{52}R_z)^{-n_{B1}} + K_{C1}(8R_z)^{-n_{C1}}}{(2R_z)^{-n_0}} + \right.$$

$$\frac{K_{D1}(\sqrt{52}R_z)^{-n_{D1}} + K_{E1}(8R_z)^{-n_{E1}} + K_{F1}(\sqrt{52}R_z)^{-n_{F1}} + K_{B2}(\sqrt{52}R_z)^{-n_{B2}}}{(2R_z)^{-n_0}} +$$

$$\left.\frac{K_{D2}(\sqrt{52}R_z)^{-n_{D2}} + K_{F2}(\sqrt{52}R_z)^{-n_{F2}}}{(2R_z)^{-n_0}}\right] \qquad (4.5)$$

Here again, the subscripts K_{A1} through K_{F1} represent the number of users in the original interfering zones of the co-channel cells as presented in Chapter III. K_{B2}, K_{D2}, and K_{F2} represent the number of users per zone of the additional interfering zones of cells B2, D2, and F2, respectively.

3. Mayer's Method for Seven-cell per Cluster Microzoning (Version Two)

The architecture and measured distances for the seven-cell per cluster microzoning system using Mayer's method (version two) are shown in Figure 4.6.

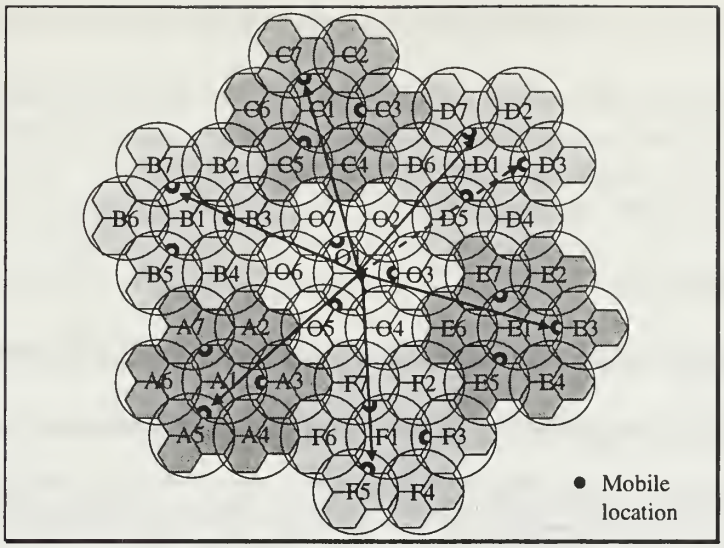

Figure 4.6: Mayer's Microzoning Method (Version Two) for a Seven-cell per Cluster System.

In the figure, the mobile unit is shown just to the right of the center of cell one of the reference cluster, falling under the control of the right-most zone of cell O1. The distances from the mobile unit to the original zone transmitters of co-channel interfering cells A1, C1, and E1 are equal with a value of $\sqrt{97}R_z$, while the distances to B1, and F1 are equal with a value of $\sqrt{91}R_z$. The distance to the original zone transmitter of cell D1 is $\sqrt{73}R_z$. In this architecture, cell D1 is the only cell that has an additional zone that could introduce interference into the reference zone of the desired cell. The distance from that zone, the top-most zone of cell D1, is $\sqrt{91}R_z$ and is denoted with a dashed line. This yields a co-channel interference term denoted by

$$\left(\frac{S}{I}\right)^{-1}_{CCI-1} = \frac{2}{3N}\left[\frac{K_{A1}\left(\sqrt{97}R_z\right)^{-n_{A1}} + K_{B1}\left(\sqrt{91}R_z\right)^{-n_{B1}} + K_{C1}\left(\sqrt{97}R_z\right)^{-n_{C1}}}{\left(2R_z\right)^{-n_0}} + \right.$$

$$\left. \frac{K_{D1}\left(\sqrt{73}R_z\right)^{-n_{D1}} + K_{E1}\left(\sqrt{97}R_z\right)^{-n_{E1}} + K_{F1}\left(\sqrt{91}R_z\right)^{-n_{F1}} + K_{D2}\left(\sqrt{91}R_z\right)^{-n_{D2}}}{\left(2R_z\right)^{-n_0}}\right] \quad (4.6)$$

Here the subscripts K_{A1} through K_{F1} represent the number of users in the original interfering zones of the co-channel cells as presented in Chapter III. K_{D2} represents the number of users in the additional interfering zone of cell D1.

D. SUMMARY

A quick reference for finding the first-tier co-channel interference equations for each of the wideband microzoning architectures is given in Table 4.1.

	One-cell per cluster	Three-cell per cluster	Seven-cell per cluster
Mayer's method Version 1	Equation 4.1	Equation 4.2	Equation 4.3
Mayer's method Version 2	Equation 4.4	Equation 4.5	Equation 4.6

Table 4.1: Equation Reference for Chapter IV Architectures

The performances of microzoning versus sectoring will be examined in the next chapter.

V. NUMERICAL ANALYSIS

Now that the expressions have been derived for the signal-to-interference plus noise ratio, specific comparisons can be performed between the different systems. For CDMA systems, analysis of the omnidirectional, sectoring, and Mayer's microzoning architectures will be presented. To enable a comparison between Lee's and Mayer's microzoning measurement methods, analysis will be performed on an FDMA system since Lee's method is only developed for FDMA. As mentioned in earlier chapters, the performance curves for all combinations of omnidirectional, 120° sectoring, and 60° sectoring architectures represent the worst case scenario. By contrast, only Mayer's microzoning method (version two) represents the true, worst case scenario for performance of the microzoning techniques examined. Performance using Lee's method and Mayer's method (version one) from the microzoning chapter are included for comparison as they do come close to representing worst case scenario analysis.

A. DERIVATIONS FOR PERFORMANCE CURVE ANALYSIS

The basic equation used for finding the signal-to-noise plus interference ratio is equation 2.1. This equation includes AWGN, intracell interference, also known as the multiuser interference within the reference cell, first-tier co-channel multiuser interference, and second-tier co-channel multiuser interference. Within the framework of a CDMA system, the multiuser interference within the reference cell is reduced to zero due to the assumption that W-H orthogonal spreading codes are used on the forward channel. Within the context of an FDMA system, there is still no multiuser interference within the reference cell, since each user within the cell operates on a different frequency.

Explicit expressions for first-tier co-channel and second-tier co-channel interference for omnidirectional and sectoring systems have been derived and listed in Chapter II. Likewise for microzoning architectures, the effects of first-tier co-channel interference have been derived for FDMA systems in Chapter III and for CDMA systems in Chapter IV.

B. SPECIFIC PARAMETERS FOR SIGNAL-TO-NOISE RATIO ANALYSIS

Specific values will be substituted for each of the parameters listed in Chapters II, III, and IV to enable a direct comparison between the different architectures by way of plots of overall S/N as a function of E_b/N_o. These variable parameters are the path loss exponent for the reference cell and the path loss exponent for each of the co-channel cells for FDMA systems. CDMA system parameters include those listed for FDMA systems as well as processing gain, number of users in the reference cell, and number of users in each co-channel cell.

Each plot in this chapter is titled with its particular frequency-reuse scheme and path loss exponent (designated as n_i) for the FDMA systems. The CDMA system plots also have those titles as well as processing gain and total number of users per cell (designated as K_i). The specific architectures shown on each plot are listed in the legend. In accordance with industry's push toward a Third Generation Standard, a processing gain of 128 is used except where otherwise indicated for comparison purposes. [7]

Of note, although the path loss exponents were kept consistent for the reference cell and all co-channels cells within each case study, the program written to produce the performance curves can accept a unique input for each path loss exponent for every cell

in either a CDMA or FDMA system. For CDMA systems, the same is true for the number of users per cell. Each cell in the system can have a different number of users. The specific cases shown were chosen to represent some typical situations without inundating the reader with endless combinations of specific values for variables.

C. PRESENTATION METHOD OF RESULTS

1. FDMA Comparisons

In this thesis, FDMA is analyzed in order to illustrate the differences between Lee's method and Mayer's methods of measuring co-channel interference in a microzoning architecture. Since Lee does not extend his method into one which can be applied to a CDMA system, several plots will be presented comparing Lee's method, Mayer's method (version one), and Mayer's method (version two) for an FDMA system. Comparisons between the three microzoning methods in one-cell, three-cell, and seven-cell per cluster layouts, respectively, for path loss exponents equal to four are shown in Figures 4.1 to 4.3. Those three microzoning architectures as well as the omnidirectional and sectoring layouts for comparison purposes in a seven-cell per cluster system are exhibited in Figure 4.4. Again, the systems in Figure 4.4 have a path loss exponent equal to four. Finally, the same six techniques presented in Figure 4.4 are shown in Figure 4.5, but using a path loss exponent equal to three.

2. CDMA Comparisons

For CDMA systems, from Figure 4.6, we see the negligible effect the second-tier co-channel interfering cells have on overall system S/N. First-tier and first- and second-tier co-channel interference are shown for omnidirectional, 120° sectoring, and 60°

sectoring in a one-cell per cluster system. A one-cell per cluster layout is chosen because it displays the largest interference contribution from second-tier co-channel cells.

Next, omnidirectional, 120° sectoring, 60° sectoring, Mayer's method (version one), and Mayer's method (version two) are compared for one-cell, three-cell, and seven-cell per cluster systems in Figures 4.7 to 4.9, respectively. The systems illustrated in Figures 4.6 to 4.9 all have path loss exponents equal to three with the number of users per cell equal to 21. The same five layouts listed above for a one-cell per cluster system with the same number of users, but path loss exponents equal to four, is shown in Figure 4.10 . The number of users was chosen to be 21 since that is the hard maximum that the 60° sectoring system can accommodate given the processing gain of 128.

The Results for omnidirectional, 120° sectoring, 60° sectoring, Mayer's method (version one), and Mayer's method (version two) for a one-cell per cluster systems are displayed in Figure 4.11. Results from using path loss exponents of three, a processing gain of 32, and number of users per cell of four are shown in these plots. With this processing gain, the bandwidth-imposed maximum number of users per cell in the 60° sectoring layout is four.

Results for a one-cell per cluster system using a processing gain of 512 and number of users per cell of 84 is demonstrated in Figure 4.12. Here too, the number of users per cell was chosen to represent the bandwidth-imposed maximum number of users per cell in the 60° sectoring layout at this processing gain.

Finally, results for omnidirectional, Mayer's method (version one), and Mayer's method (version two) for the one-cell per cluster pattern, using the original processing gain of 128, path loss exponents of three, and users per cell/zone of 125 are shown in

Figure 4.13. The 120° and 60° sectoring schemes are not included in this plot since their bandwidth-imposed maximum number of users per cell at this processing gain are 42 and 21, respectively.

D. INTERPRETATION OF RESULTS

1. FDMA Microzoning Results

For the three-cell and seven-cell per cluster layouts, Mayer's method (version one) yields the best performance, followed by Lee's method, with Mayer's method (version two) coming in last. This is to be expected since Mayer's method (version two) is the only true worst case scenario of the three microzoning techniques. This can be seen in Figures 4.2 and 4.3.

For the one-cell per cluster microzoning layouts, however, performance from best to worst is as follows: Mayer's method (version one), Mayer's method (version two), and Lee's method. This can be seen in Figure 4.1. Because the one-cell per cluster case is the most geographically compact architecture in terms of the distance to the co-channel cells, the improvement due to better accuracy in measuring distance to the actual interfering transmitter's location has the greatest effect in this layout. The additional distance that results from the difference in directionality and transmitter placement between Lee's method and Mayer's methods produces a significant increase, percentage-wise, of the co-channel interfering distance. In the one-cell per cluster architecture, the advantage is great enough to overcome the disadvantage of having a true worst case mobile location, as in Mayer's method (version two). As a result, Mayer's method (version two) is still a more accurate measurement of worst case S/N than Lee's method,

even though the latter is not a true worst case representation. In other words, for the one-cell per cluster layout, Mayer's method (version two) is a more accurate representation of the worst case scenario, while still showing the performance of microzoning to be better than previously analyzed in Lee's method by about 2.5 dB at an E_b/N_o of 25 dB.

When compared against omnidirectional and sectoring antennas in a seven-cell per cluster system as in Figure 4.4, the results from best to worst are as follows: Mayer's microzoning method (version one), 60° sectoring, Lee's microzoning method, 120° sectoring, Mayer's microzoning method (version two), and finally, the omnidirectional layout. At an E_b/N_o of 20 dB, Mayer's microzoning method (version one), 60° sectoring, Lee's microzoning method, and 120° sectoring are within 1.5 dB of each other. At that E_b/N_o, all six methods are within about 4.0 dB of each other. As the E_b/N_o is increased to 25 dB in the seven-cell per cluster system, there is about 7.0 dB of difference between the best performer, Mayer's microzoning method (version one), and the worst performer, the omnidirectional layout. As previously established, Mayer's microzoning method (version one) may present a slightly optimistic S/N measurement since the mobile's location is based upon Lee's published mobile placement. The difference between Mayer's method (version one) and the 60° sectoring architecture at an E_b/N_o of 20 dB is a couple tenths of a dB. The difference between Mayer's method (version one) and the 120° sectoring architecture is about 1.5 dB. Lee's method in this comparison offers no real value, since the measurement technique is not accurate. It is just offered as a springboard to get to Mayer's methods. Recall Mayer's method (version two) is a conservative estimate of the worst case location and is shown as having a value about 2.0 dB less than the 120° sectoring architecture at an E_b/N_o of 20 dB.

Given the relatively close performance of the six methods evaluated, 120° sectoring is probably a better choice than 60° sectoring in an FDMA system due to the added hardware costs and lowered trunking efficiency associated with 60° sectoring. However, realizing that the worst case scenario for microzoning measurement lies somewhere between the optimistic Mayer's method (version one) and the pessimistic Mayer's method (version two), microzoning is perhaps the most attractive candidate for use in an FDMA system. Since the S/N of the different interference reduction methods is relatively close, the collateral benefits of microzoning such as the preservation of trunking efficiency, thereby allowing for greater user capacity, and soft hand-off make it the better choice. There is also no additional overhead associated with frequency assignment planning within the sectors of each cell as there is with the sectoring schemes.

A seven-cell per cluster system was chosen for the previous comparison because it is the most widely used layout for FDMA systems. For frequency-reuse patterns less than seven, the co-channel interference is generally too high to allow for a satisfactory S/N of approximately 18 dB. [3] Of note, Mayer's method (version one), though optimistic, shows some potential in the three-cell per cluster system by exhibiting a value of 18.8 dB at an E_b/N_o of 20 dB.

When the path loss exponents are reduced, as in Figure 4.5, the performances all show degradation. In such an environment, the difference between Mayer's method (version one) and 60° sectoring is virtually indistinguishable. These values are about 2.0 dB lower than they were with the path loss exponent equal to three. Additionally, for the lower path loss exponent, there is slightly more than a 2.0 dB difference between 60° sectoring and 120° sectoring. Since the cases presented here assign the same path loss

exponent to the reference cell and all the co-channel cells, the penalty for having a higher path loss exponent in the reference cell is outweighed by the fact that all of the interfering cells also have a higher path loss exponent. This results in more attenuation of the transmissions from the co-channel cells, and hence, lowers interference.

2. CDMA Results

The trend observed for the omnidirectional and sectoring layouts is that the S/N of each CDMA system from best to worst always follows the same pattern: first-tier 60° sectoring, first- and second-tier 60° sectoring, first-tier 120° sectoring, first- and second-tier 120° sectoring, first-tier omnidirectional use, and finally, first- and second-tier omnidirectional use as seen in Figure 4.6. This follows intuition, since the smaller the sector, the fewer users there are to generate interference into the reference cell. The difference between the S/N generated when considering first-tier only and the combination of first- and second-tier interference is at a maximum in the one-cell per cluster cases, where there is a fraction of a dB of difference. As the frequency-reuse patterns increase, the differences between the S/N ratios due to the first-tier and the combination of first- and second-tier interference become almost indistinguishable. These results show that the second-tier interferers have a minor effect on the S/N ratio when compared to the directivity of the antenna and the frequency-reuse factor.

The comparison between Mayer's microzoning method (version one), 60° sectoring, Lee's microzoning method, 120° sectoring, Mayer's microzoning method (version two), and the omnidirectional layout for one-cell, three-cell, and seven-cell per cluster architectures, respectively, are shown in Figures 4.7 to 4.9. Mayer's microzoning method (version one) exhibits the best performance of 17.9 dB at an E_b/N_o of 25 dB,

followed by Mayer's microzoning method (version two) at 15.1 dB, 60° sectoring at 13.3 dB, 120° sectoring at 10.5 dB, and finally, omnidirectional antenna use at 5.9 dB. The differences between methods are less pronounced in the higher frequency-reuse patterns. For the three-cell per cluster system at an E_b/N_o of 25 dB, the performance order is: Mayer's method (version one) at 24 dB, 60° sectoring at 20.8 dB, Mayer's method (version two) at 20.1 dB, 120° sectoring at 18.3 dB, and finally, the omnidirectional system at 14.8 dB. In the seven-cell per cluster system, the performance at an E_b/N_o of 25 dB is as follows: Mayer's method (version one) at 25 dB, 60° sectoring at 23.5 dB, Mayer's method (version two) at 22.6 dB, 120° sectoring at 22.5 dB, and finally, the omnidirectional system at 19.8 dB. As expected, the omnidirectional antenna scheme shows the most improvement as the frequency-reuse pattern is increased. However, the modest S/N improvements experienced by all systems utilizing higher frequency-reuse patterns is not sufficient enough to warrant the associated data rate reduction nor the overhead accompanying the division of the spectrum into sub-bands.

The advantages of microzoning's ability to reuse the same codes within different zones of the same cell and soft hand-off capability in addition to its better performance in the one-cell per cluster case make it a better option than sectoring in a CDMA system. Additionally, there is no need for careful code assignment or distribution of codes amongst the different sectors within a cell as there is with sectoring. This eliminates extensive and difficult code-reuse planning.

The effects of raising the path loss exponent from three to four is shown in Figure 4.10. As was the case with the FDMA systems, the higher path loss exponent actually improves the results slightly. At an E_b/N_o of 25 dB, the microzoning methods show

improvements of 3.0 to 3.5 dB, while the sectoring and omnidirectional schemes show about 0.5 to 1.0 dB of improvement. The greater the path loss exponents, the less effect the potential interfering zones have on the overall S/N.

The main effect experienced from adjusting the system processing gain is the change in the bandwidth-imposed maximum number of users. When comparing a system with a processing gain of 32 and four users per cell as shown in Figure 4.11 against a system with a processing gain of 512 and 84 users per cell as shown in Figure 4.12, the S/N of each method varies less than one dB from one processing gain to another. This is a reasonable result since both systems are operating at the bandwidth-imposed maximum number of users for the 60° sectoring case at their respective processing gains.

As expected, the larger the processing gain, the more users per cell that can be supported at the same S/N. However, it is unlikely the Third Generation Wireless Standard will employ a processing gain greater than 128. [7]

As expected for all architectures, the best performance occurs with the least number of users per cell. Typically, the intra-cell interference due to multiple users operating within the same cell is the limiting factor in the number of users per cell a system can support. However, since we are using W-H orthogonal spreading codes on the forward channel, the intra-cell interference is assumed to be zero. As a result, our system can accommodate many more users than perhaps anticipated.

The microzoning and omnidirectional architectures for 125 users per cell is illustrated in Figure 4.13. Here, 60° and 120° sectoring are not shown because those methods cannot support that number of users. As previously mentioned, the 60° sectoring system can only support 21 users, while the 120° sectoring method can only

support 42 users at a processing gain of 128. By contrast, microzoning systems can utilize all 125 available forward channels provided the S/N supports it. As developed in the Third Generation Standard, a S/N of approximately 5 to 10 dB is desired. [5] We find that both of Mayer's microzoning measurement methods fall between about 7.5 and 11.0 dB at an E_b/N_o of 25 dB. By contrast, the omnidirectional scheme exhibits an S/N of –2.0 dB. Hence, microzoning is a desirable method for keeping the S/N within acceptable levels while allowing many more users than the sectoring methods. The additional benefit of soft-handoff related to the microzoning method makes it particularly attractive for use in a CDMA system.

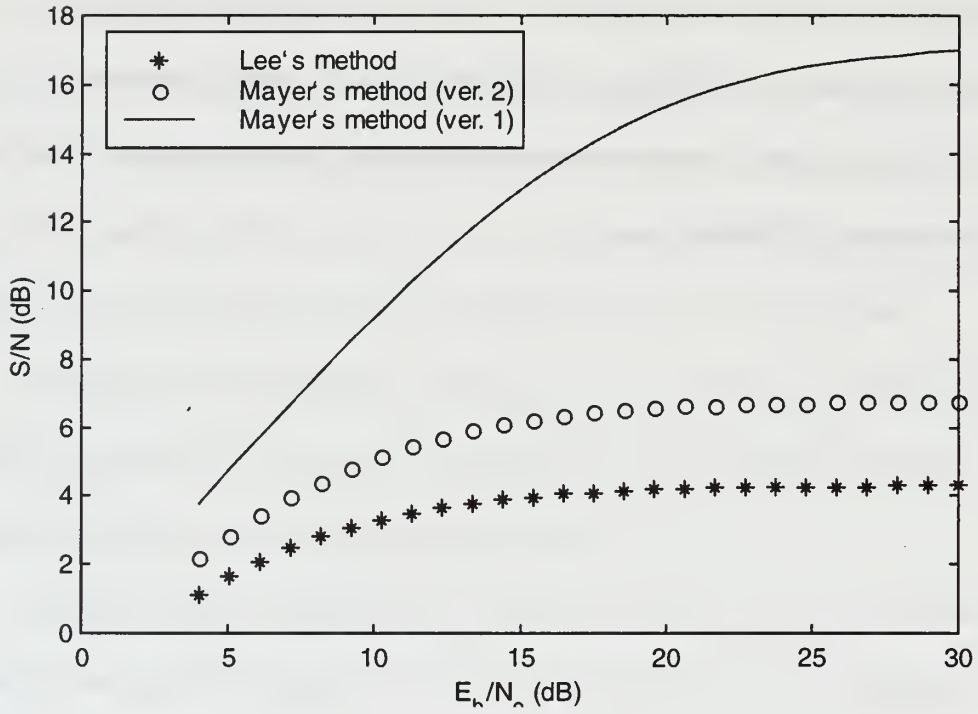

Figure 5.1: One-cell per Cluster FDMA Microzoning with $n_i = 4$.

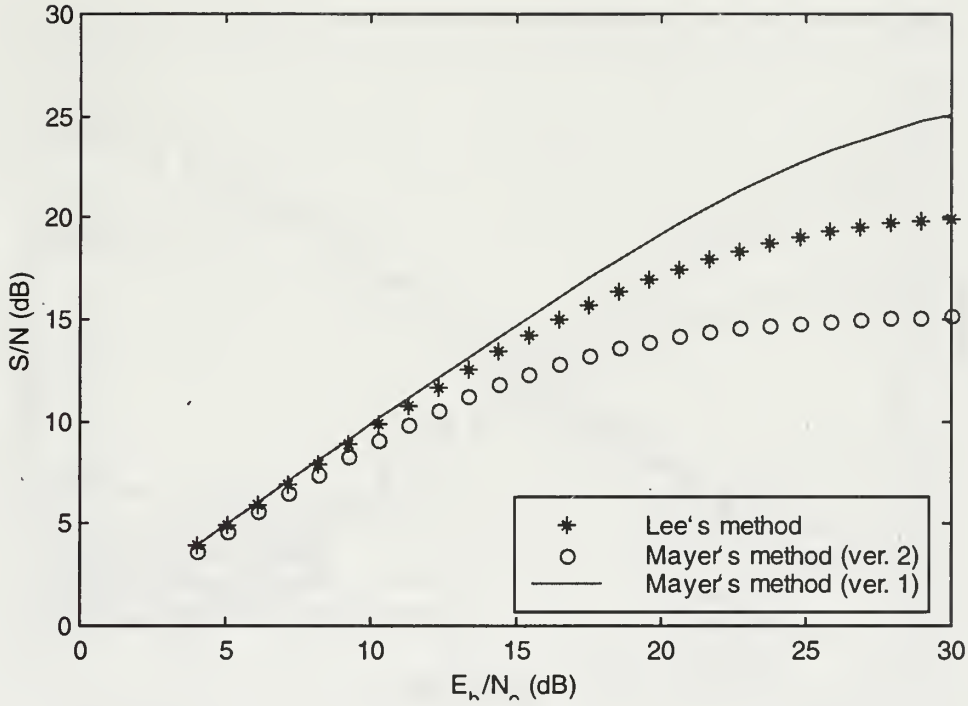

Figure 5.2: Three-cell per Cluster FDMA Microzoning with $n_i = 4$.

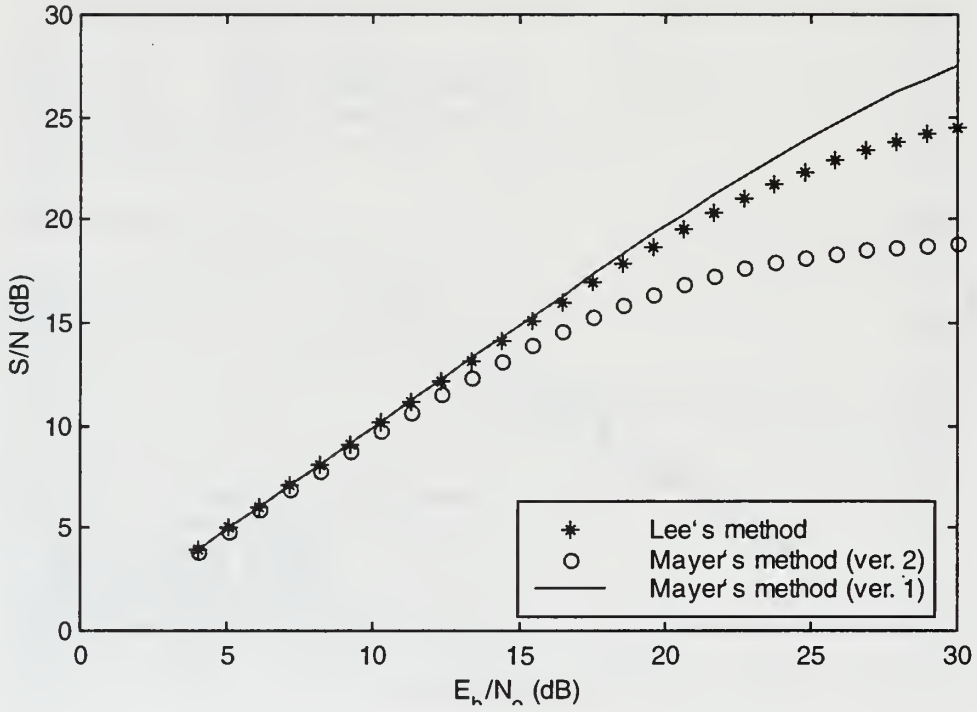

Figure 5.3: Seven-cell per Cluster FDMA Microzoning with $n_i = 4$.

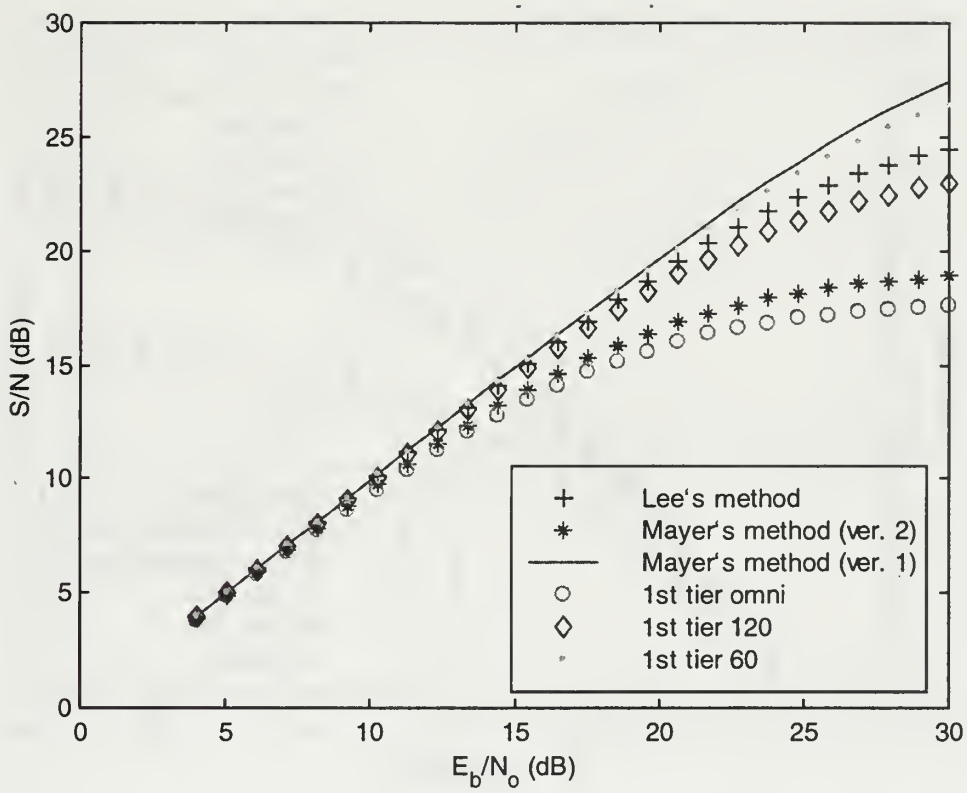

Figure 5.4: Seven-cell per Cluster FDMA System Comparison with $n_i = 4$.

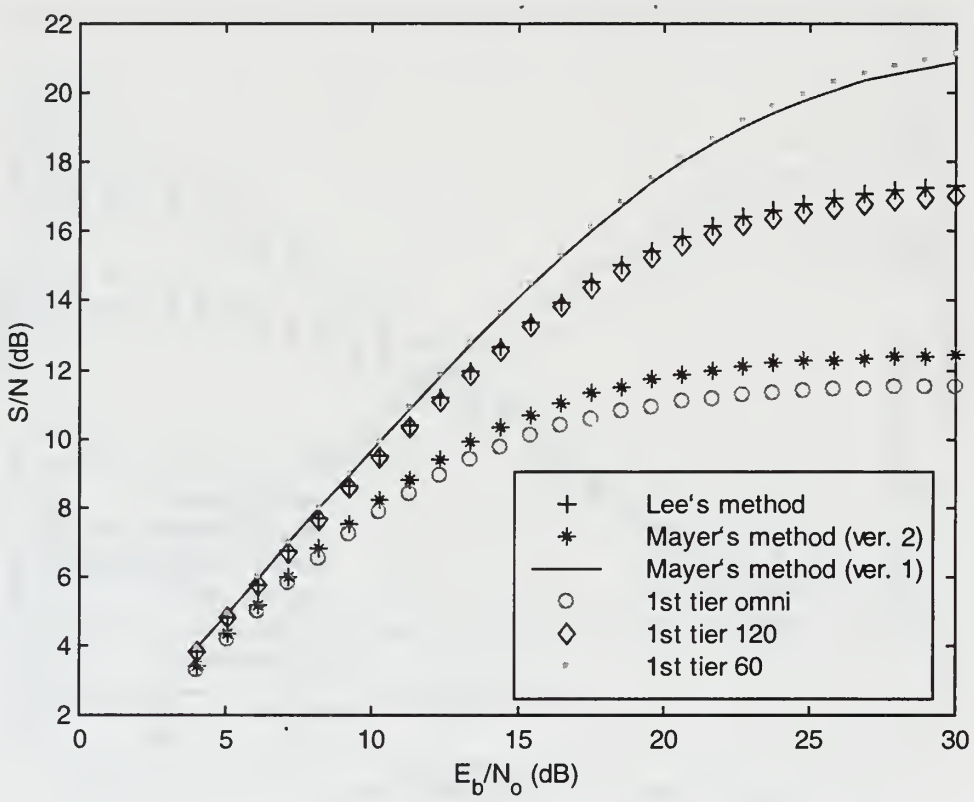

Figure 5.5: Seven-cell per Cluster FDMA System Comparison with $n_i = 3$.

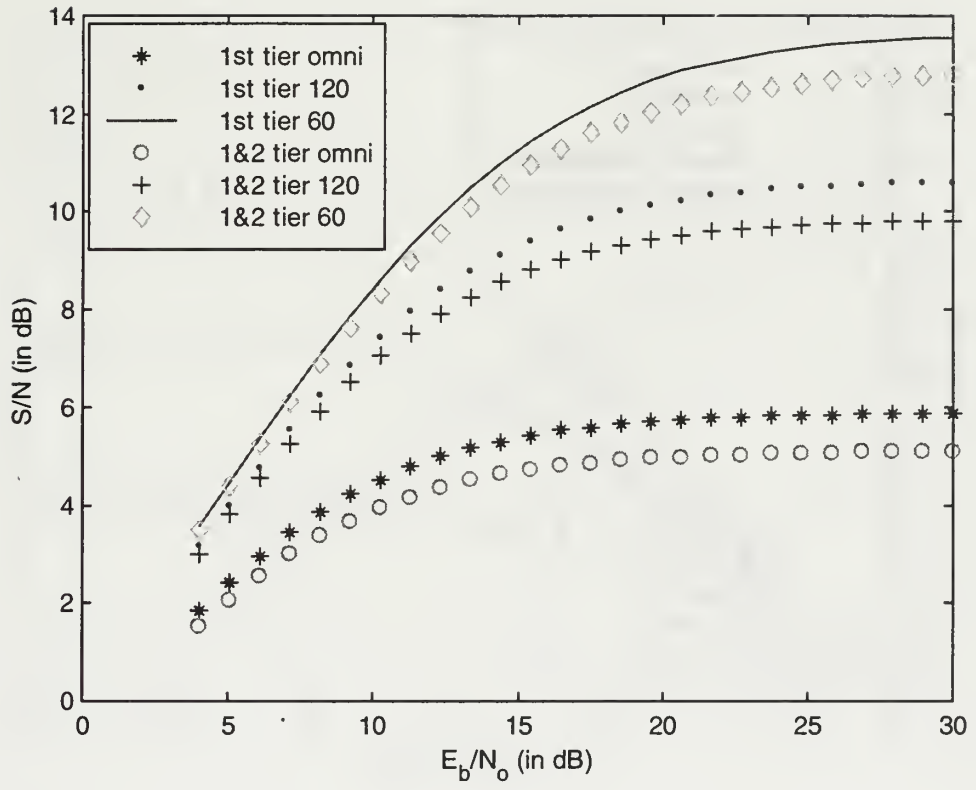

Figure 5.6: First- and Second-tier Co-Channel Interference for a One-cell per Cluster CDMA System with Processing Gain of 128, $n_i = 3$, and $K_i = 21$.

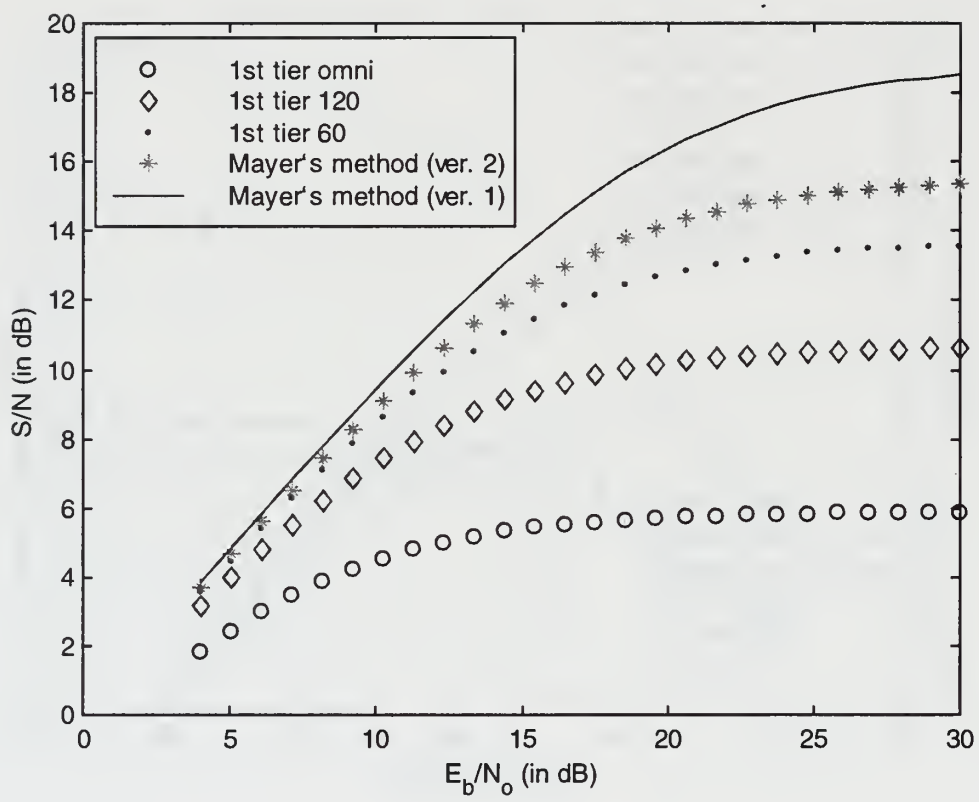

Figure 5.7: One-cell per Cluster CDMA System Comparison with Processing Gain of 128, $n_i = 3$, and $K_i = 21$.

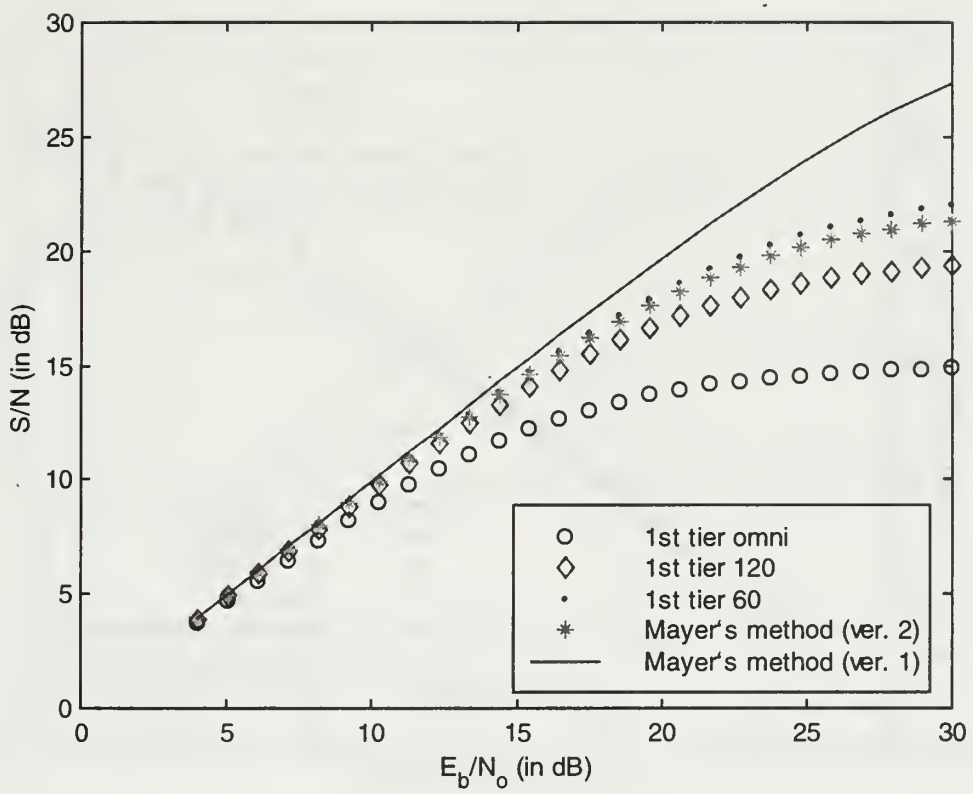

Figure 5.8: Three-cell per Cluster CDMA System Comparison with Processing Gain of 128, $n_i = 3$, and $K_i = 21$.

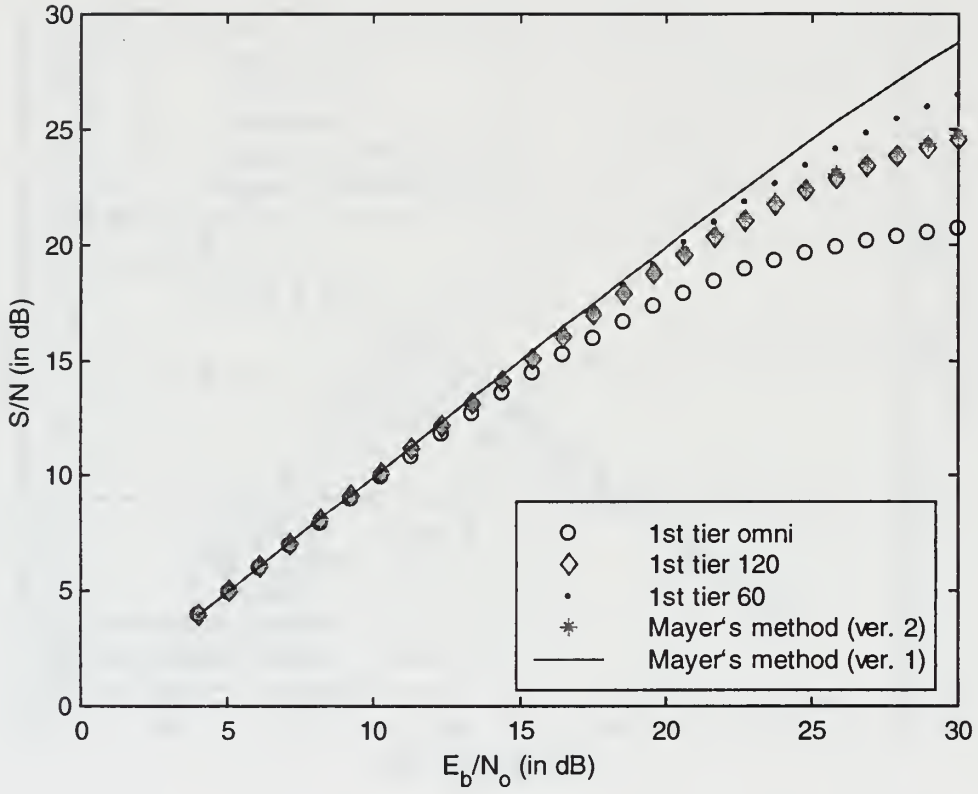

Figure 5.9: Seven-cell per Cluster CDMA System Comparison with Processing Gain of 128, $n_i = 3$, and $K_i = 21$.

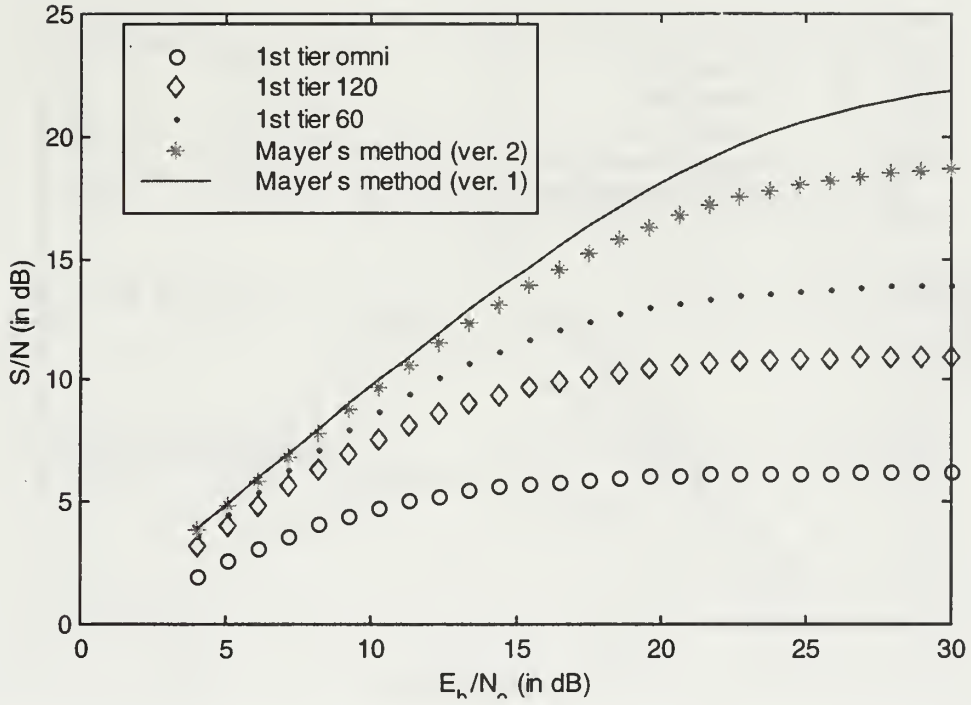

Figure 5.10: One-cell per Cluster CDMA System Comparison with Processing Gain of 128, $n_i = 4$, and $K_i = 21$.

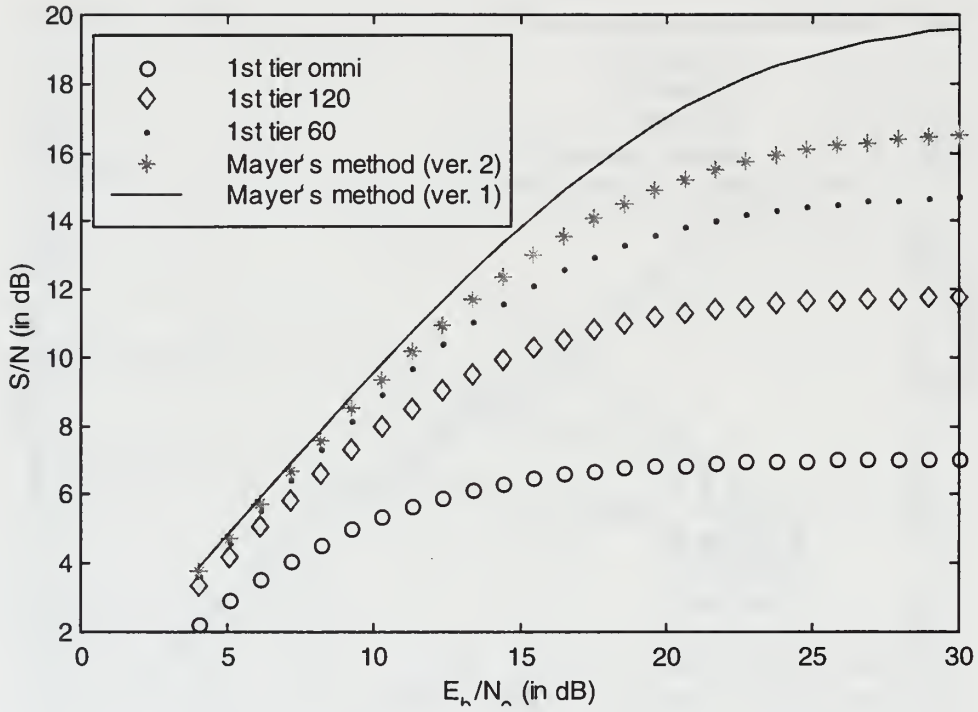

Figure 5.11: One-cell per Cluster CDMA System Comparison with Processing Gain of 32, $n_i = 3$, and $K_i = 4$.

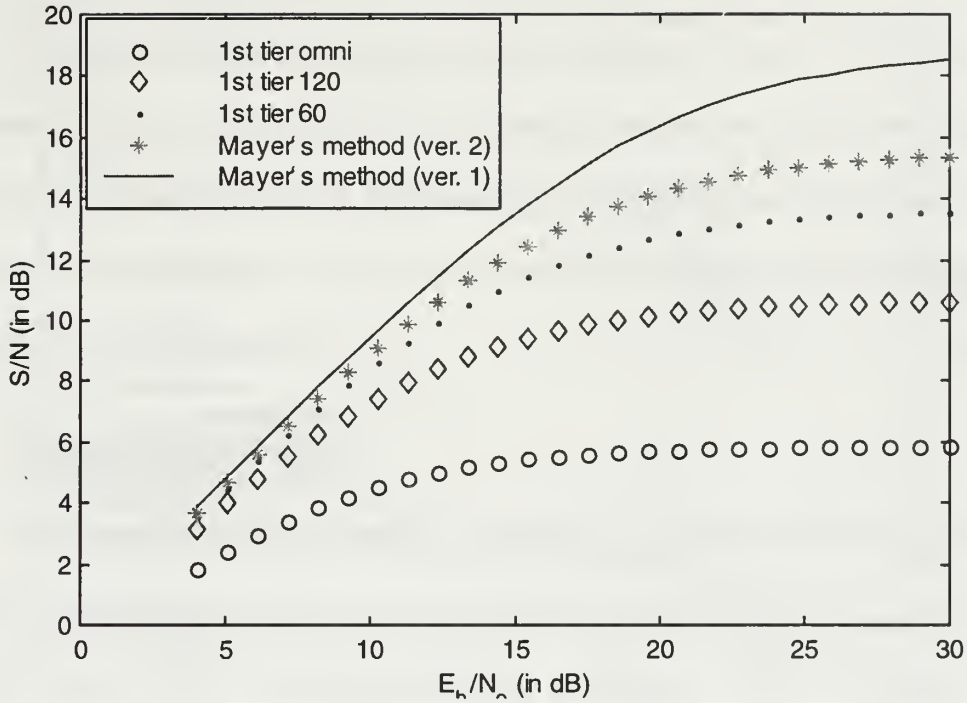

Figure 5.12: One-cell per Cluster CDMA System Comparison with Processing Gain of 512, $n_i = 3$, and $K_i = 84$.

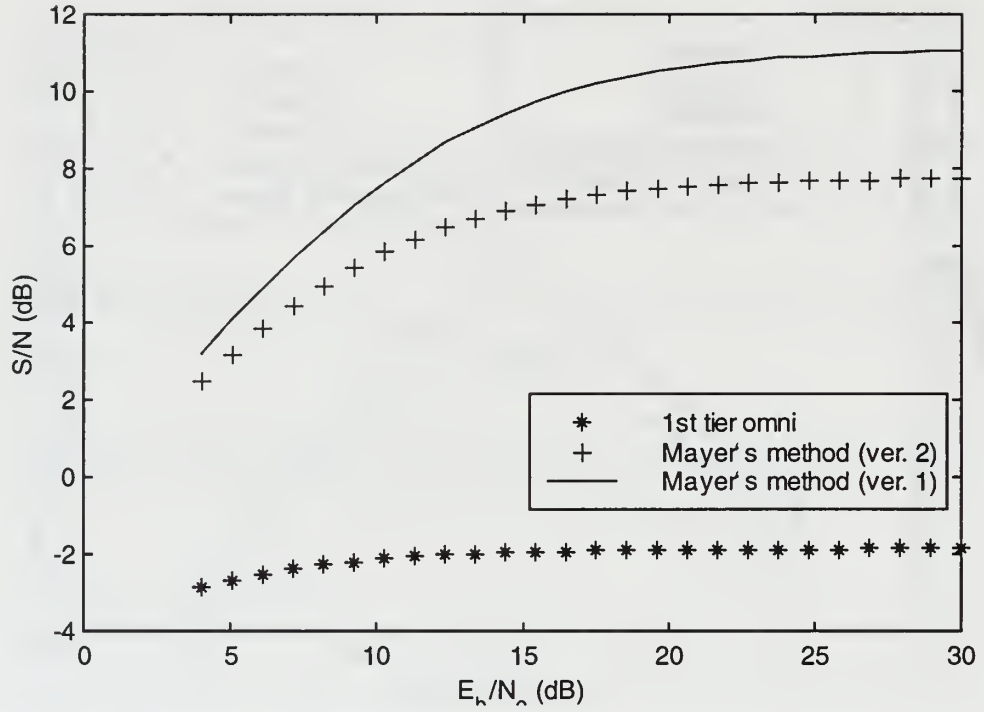

Figure 5.13: One-cell per Cluster CDMA System Comparison with Processing Gain of 128, $n_i = 3$, and $K_i = 125$.

VI. CONCLUSION

In order to support the explosive growth rate of multimedia mobile communications, new technologies must be developed to provide reliable, high data rate services. Of the multiple access techniques used in cellular communications, CDMA is the front-runner for this third generation of wireless communications.

The primary restriction on performance in this type of system is the co-channel interference. Its reduction equates to better quality of service and greater user capacity. Several different architectures for implementing such a system have been presented, in addition to an investigation of the published inaccuracies in one interference reduction method known as microzoning.

A. FDMA CONCLUSIONS

The three methods examined for microzoning in an FDMA system are Lee's method, Mayer's method (version one) and Mayer's method (version two). Mayer's method (version two) is the only true worst case investigation of S/N of the three methods. It corrects the previous erroneous analysis published by Lee. [4]. When compared with 120° and 60° sectoring methods, the performance of Mayer's microzoning (version two) performs at a slightly lower S/N. However, its performance still shows improvement over that of the omnidirectional case. The benefits of microzoning over sectoring in an FDMA system include soft hand-off and preservation of trunking efficiency, which allows for greater capacity. Another advantage is that there is no need for additional frequency assignment planning within the sectors of each cell as

there is with sectoring schemes. These factors outweigh the slight disadvantage in S/N experienced by microzoning, making it the better choice for use in FDMA systems.

B. CDMA CONCLUSIONS

The interference reduction methods examined for CDMA are higher frequency-reuse patterns, sectoring, and microzoning. The use of higher frequency-reuse patterns proves not to be a good choice. Although there is some S/N improvement associated with its use, it is not sufficient enough to overcome the accompanying data rate reduction. There is also additional overhead related to the frequency planning necessary when dividing the available spectrum into sub-bands.

Although sectoring does show significant improvement over the omnidirectional scheme, it does not exhibit as great of an improvement as the microzoning schemes do. Additionally, there are several disadvantages associated with sectoring, including a reduction of capacity and hard hand-off. The capacity reduction factor is six for 60° sectoring and three for 120° sectoring. The accompanying code distribution planning is another burden for these methods.

In addition to higher S/N, microzoning provides for soft hand-off between zones of a cell. Also, there is no need for the extensive and difficult task of code-reuse planning, which is one of the original advantages to choosing a CDMA system to implement the Third Generation Standard in the first place. These factors coupled with its performance make microzoning the most promising candidate for providing the necessary interference reduction to enable the operation of the next generation high data rate cellular system.

LIST OF REFERENCES

1. Dinan, E., Jabbari, B., "Spreading Codes for Direct Sequence CDMA and Wideband CDMA Cellular Networks", *IEEE Communications Magazine*, September 1998.

2. Adachi, F., "Theoretical Analysis of DS-CDMA Reverse Link Capacity with SIR-Based Transmit Power Control", *IEICE Transactions on Fundamentals of Electronics, Communications, and Computer Sciences*, Vol. E79-A, No. 12, December 1996.

3. Rappaport, T., *Wireless Communications: Principles and Practice,* Prentice Hall, Upper Saddle River, NJ, 1996.

4. Lee, W., "Smaller Cells for Greater Performance", *IEEE Communications Magazine*, November 1991.

5. Adachi, F., Sawahashi, M., Suda, H., "Wideband DS-CDMA for Next-Generation Mobile Communications Systems", *IEEE Communications Magazine*, September 1998.

6. Pursley, M. B., Sarwate, D. V., Stark, W. E., "Performance Evaluation for Phase-Coded Spread Spectrum Multiple-Access Communication – Part II: Code Sequence Analysis", *IEEE Transactions on Communications*, Vol. COM-25, No. 8, August 1987.

7. Dahlman, E., Gudmundson, B., Nilsson, M., Skold, J., "UMTS/IMT-2000 Based on Wideband CDMA", *IEEE Communications Magazine*, September 1998.

INITIAL DISTRIBUTION LIST

No. Copies

1. Defense Technical Information Center.....2
   8725 John J. Kingman Rd., STE 0944
   Ft. Belvoir, VA 22060-6218

2. Dudley Knox Library.....2
   Naval Postgraduate School
   411 Dyer Rd.
   Monterey, CA 93943-5101

3. Chairman, Code EC.....1
   Department of Electrical and Computer Engineering
   Naval Postgraduate School
   Monterey, CA 93943-5121

4. Professor Tri Ha, Code EC/Ha.....2
   Department of Electrical and Computer Engineering
   Naval Postgraduate School
   Monterey, CA 93943-5121

5. Professor R. Clark Robertson, Code EC/Rc.....2
   Department of Electrical and Computer Engineering
   Naval Postgraduate School
   Monterey, CA 93943-5121

6. LT Tanya Mayer.....3
   6207 S. Osborne Rd.
   Upper Marlboro, MD 20772